To the Graduate Council:

I am submitting herewith a thesis written by Gregory Darin Hollis entitled "The Reduction of Scale Force Uncertainty in Low Thrust Regions." I have examined the final copy of this thesis for form and content and recommend that it be accepted in partial fulfillment of the requirements for the degree of Master of Science, with a major in Mechanical Engineering.

Roy J. Schulz

Dr. Roy Schulz, Major Professor

We have read this thesis
and recommend its acceptance

Accepted for the Council:

Associate Vice Chancellor and
Dean of the Graduate School

The Reduction of Scale Force Uncertainty in Low Thrust Regions

A Thesis
Presented for the
Master of Science
Degree

The University of Tennessee, Knoxville

Gregory Darin Hollis
December 1997

Distribution Unlimited

DEDICATION

This thesis is dedicated to my family

Mr. Joseph Dixon Hollis,

Mrs. Lucy Baskin Hollis,

Mrs. Michelle Hollis Keller,

and

Mr. Jeffery Dixon Hollis

who have given me the courage to further my education.

ACKNOWLEDGMENTS

There are many people to whom I am grateful for making this achievement possible. I have benefited greatly from the support and knowledge of my co-workers: Art Mantone, Larry Oneal, Roy Thompson, Wade Burfitt, and Jim Childers. They have all read a number of revisions of the thesis and the merit of this work is due in no small part to their suggestions. I have grown to respect these individuals over the last four years, and hope that these relationships will endure.

There are a number of other people whose assistance should be recognized. I would like to thank Jeff Albro, Dr. Virgil Smith, Dr. Roy Schulz, Dr. Ching Lo, and Dr. Ahmad Vakili. Without their valuable time and generous support, the culmination of this project would not have been possible.

ABSTRACT

Minimal scale force uncertainty in low thrust regions of an engine's operating envelope is critical to meet flight test specifications as Air Force requirements become more stringent. In these low thrust regions, scale force accounts for over 90% of the total thrust uncertainty. Through experiments and experience, the elemental errors associated with scale force uncertainty have proven to be reducible. The primary contributors to scale force uncertainty in low thrust regions include such errors as thrust stand/load cell hysteresis and pre- to post-test zero shifts. Cell heating effects are also very important because they affect the test cell environment where scale force measurements are obtained. During engine altitude development testing in the C1 Altitude Test Facility at Arnold Engineering and Development Center (AEDC), these contributors were evaluated in an effort to obtain uncertainty levels of less than 1%. To date, data have been collected via thrust stand calibrations, cell temperature correlations, and pre- to post-test load cell readings.

A root-sum-square uncertainty analysis was used to evaluate five operating scenarios to determine the optimal procedures for low scale force uncertainty at the 3,000 lbf scale force level. The five operating scenarios were derived from experimental efforts to reduce hysteresis and zero shifts. The results show that scale force uncertainty levels can be reduced to 0.74% of 3,000 lbf, down from an initial level of 2.41% of 3,000 lbf.

With these results, operating procedures for thrust stand calibrations and temperature limits on the test cell environment were obtained.

Table of Contents

Part Page

1. Introduction 1
   - 1.1 Definition of Uncertainty Measurements 2
     - 1.1.1 Elemental Errors 2
       - 1.1.1.1 Bias Errors 3
       - 1.1.1.2 Precision Errors 4
   - 1.2 Propagation of Bias and Precision Errors in Uncertainty 5
   - 1.3 Thrust Elemental Errors 6

2. Elemental Error Reduction 10
   - 2.1 The Test Environment in an Altitude Simulating Test Cell 11
   - 2.2 Effects on Scale Force Measurement 13
     - 2.2.1 Hysteresis Effects 16
       - 2.2.1.1 Thrust Stand Calibration Experiments 17
     - 2.2.2 Thermal Effects 24
     - 2.2.3 Zero Shift Effects 27
     - 2.2.4 Data System Effects 29
   - 2.3 Future Work 31

3. Methods and Analytical Results 34
   - 3.1 Analysis Methodology 35
   - 3.2 Scale Force Uncertainty Analysis 38
     - 3.2.1 Analysis 1 38
     - 3.2.2 Analysis 2 39
     - 3.2.3 Analysis 3 40
     - 3.2.4 Analysis 4 43
     - 3.2.5 Analysis 5 45

4. Conclusion and Recommendations 49
   - 4.1 Summary 50

Table of Contents (Continued)

Part Page

4.2 Control of Hysteresis Effects 50
4.3 Control of Thermal Effects and Zero Shifts 51
4.4 Recommendations 54

References 57

Appendices 59
Glossary of Terms 60
Appendix A. "Theoretical Combination of Elemental Errors 63
Appendix B. "Definition of Thrust Terms" 66
Appendix C. "Thrust Stand Calibrations" 69
Appendix D. "Curve-Fit Error" 74
Appendix E. "Zero Shift Error" 77
Appendix F. "Implications of Thermal Growth of Test Cell on Zero Shifts" 80
Vita 83

List of Tables

Table Page

1. Scale Force Elemental Errors 8
2. Results of Analysis 1 of Elemental Errors on Scale Force Uncertainty 37
3. Results of Analysis 2 of Reduced Elemental Errors on Scale Force Uncertainty 41
4. Results of Analysis 3 of Reduced Elemental Errors on Scale Force Uncertainty 42
5. Results of Analysis 4 of Reduced Elemental Errors on Scale Force Uncertainty 44
6. Results of Analysis 5 of Reduced Elemental Errors on Scale Force Uncertainty 46
7. Analysis Summary 48

C.1 Conventional Thrust Stand Calibration 70
C.2 50K Thrust-Side-Only Calibration 71
C.3 10K Thrust-Side-Only Calibration 72
C.4 +30K to -10K Thrust Stand Calibration 73

List of Figures

Figure Page

1. Typical Engine Flight Envelope....12
2. Turbine Engine Test Cell....14
3. Turbine Engine Thrust Stand....15
4. Positive 50K Cal vs. Conventional Cal....19
5. 10K Cal vs. Conventional Cal....21
6. +30K to -10K Cal vs. Conventional Cal....23
7. Zero Shift History....30
8. Curve-Fit Error....76
9. Zero Shift Error....79

Nomenclature

α	thermal expansion coefficient
ζ	thermal growth
Δ	delta, change in reading
A_2	engine inlet area
A_9	engine exit area
B	overall bias error
$B_{1,2,3}$	bias errors in measurement categories 1,2, and 3 respectively
$B_{11...33}$	elemental bias measurement errors
DP	data point
E	modulus of elasticity
F	force
F_G	gross engine thrust
F_N	net/uninstalled engine thrust
F_{Ram}	inlet momentum/drag force
F_S	scale force
FAC	calibrate load cell force
g	gravitational constant
I	moment of inertia
L	length
m_{Fuel}	mass of engine fuel
m_2	mass of engine inlet air
m_9	mass of engine exhaust air
P_0	ambient static pressure
P_2	engine inlet static pressure
P_9	engine exhaust static pressure
S	overall precision error
$S_{1,2,3}$	precision errors in measurement categories 1,2, and 3 respectively
$S_{11...33}$	elemental precision measurement errors
U_{rss}	root-sum-square uncertainty method
U_{add}	additive uncertainty method
V_0	free stream air velocity
V_2	engine inlet air velocity

Nomenclature (Continued)

V_9	engine exhaust velocity
y	deflection

Abbreviations

AEDC	Arnold Engineering and Development Center
AISI	American Iron and Steel Institute
PMEL	Precision Measurements Equipment Lab
NIST	National Institute of Standards and Technology
C1	Test Facility at AEDC

PART 1

INTRODUCTION

"When you can measure what you are speaking about, and express it in numbers, you know something about it; when you cannot express it in numbers, your knowledge is of a meager and unsatisfactory kind" Lord Kelvin [2]

1.1 Definition of Uncertainty Measurements

Uncertainty is an inevitable part of every measurement taken. Formally, it represents a reasonable expectation as to the largest error possible for a measurement process [1]. The measurement process involves all facets of instrumentation, from calibration procedures and signal conditioning equipment, to external factors, such as thermal effects, and data reduction equipment. As a result, every one of these measurement aspects contribute to the total error, or uncertainty, and are defined as elemental errors [1]. The focus of this paper concerns the development of test and calibration procedures to minimize the contributions of elemental errors to scale force uncertainty.

1.1.1 Elemental Errors

There are two classifications of elemental errors that are dealt with when performing uncertainty calculations : Bias errors (B) and Precision errors (S). Total error or total uncertainty of a measurement process is simply a combination of these errors. There are currently two methods of combining these errors: the additive method (U_{ADD}) and the root-sum-square method (U_{RSS}). U_{ADD} is simply an addition of these errors, while U_{RSS} is the square root of the sum of the errors squared. Either method is acceptable, but

the U_{RSS} method will be used here because it is the selected method of AEDC. Further discussion on this method will be presented in a later section. Appendix A discusses the theoretical combination of elemental errors in overall system uncertainty through the use of the Taylor series [3].

1.1.1.1 Bias Errors

Bias error is defined as the difference between the mean of the observed measurements and the true value of a given parameter. Biases are introduced by some misaligned or defective instrument over the range of an experiment and remain fixed or consistent. There are five types of bias errors [2]:

1. Large with known magnitude and sign
2. Small with known magnitude and sign
3. Large with unknown magnitude and unknown sign
4. Small with unknown magnitude and known sign
5. Small with unknown magnitude and unknown sign

The bias errors for each component obtained during calibration, data acquisition, and data reduction are first combined by the root-sum-square method, and the measurement bias uncertainty computed through the same method, as follows:

$$B_1 = [(B_{11})^2 + (B_{21})^2 + (B_{31})^2]^{1/2}$$

$$B_2 = [(B_{12})^2 + (B_{22})^2 + (B_{32})^2]^{1/2}$$

$$B_3 = [(B_{13})^2 + (B_{23})^2 + (B_{33})^2]^{1/2}$$

which yields $B = [(B_1)^2 + (B_2)^2 + (B_3)^2]^{1/2}$

where B_1 ,B_2 , and B_3 are the basic root-sum-square errors of the three categories being considered, and B_{11}, B_{12}, ... , B_{33} are elemental bias errors.

1.1.1.2 Precision Errors

Precision error is defined as the standard deviation about a mean value. These types of errors are random or variable and always follow some statistical distribution. These random errors are due to many small, independent effects which usually cannot be identified or controlled. Through repeated measurements, the data will reveal a scatter about a mean value. This mean value is assumed to be the true, yet biased, value. In the history of uncertainty analyses, it has been found that the statistical distribution of many parameters about their mean values obtained from repeated measurements, follow what is called a "students 't' distribution." Through the use of this 't' distribution, statistics can be applied to quantify the precision error as it relates to scale force uncertainty. For a complete review of this methodology, see Reference [3].

The precision error is obtained in the same manner as the bias error such that:

$$S = [(S_1)^2 + (S_2)^2 + (S_3)^2]^{1/2}$$

where S_1, S_2, and S_3 are the basic root-sum-square errors of the three categories being considered.

1.2 Propagation of Bias and Precision Errors into Uncertainty

Once the bias and precision errors of a measurement process are computed and defined, they are used to assign the overall uncertainty of the measurements. For cases where the desired results are measured directly, calculation of uncertainty is not a problem, but in nearly all other experiments, it is necessary to compute the uncertainty in the results from the estimates of the uncertainty in the basic measurements. This computation process is called "propagation of uncertainty"[4]. The computation process is designed to insure that the final results of uncertainty are as accurate as the elemental errors. Reference [4] describes two rules of thumb that are important to note here: (i) When two uncertainties are combined and one is three or more times larger than the other, the smaller uncertainty has negligible effect, (ii) When a large number of uncertainties, say six or more, are combined, any uncertainty less than one-fifth of the largest uncertainty will have negligible effect.

Uncertainty propagation involves the reduction and evaluation of classes or sets of derivatives, which is central to the whole procedure. Data reduction techniques have been developed for evaluation using computers, based on parameter perturbations that are fed into the differentials that result from the data reduction equations, which are explained in reference [5]. References [4] and [5] give some examples.

After the uncertainty propagation has been done, the uncertainty limit for each parameter can be calculated. As mentioned earlier, two methods to calculate total uncertainty U_{ADD} or U_{RSS} are available. These two methods are:

$$U_{ADD} = \pm (B + T_{95}S)$$

or, $$U_{RSS} = \pm (B^2 + (T_{95}S)^2)^{1/2}$$

For random samples with more than about 30 measurements, T_{95} can be safely approximated as 2. As previously mentioned, the U_{RSS} methodology will be used to evaluate the measurement uncertainty on scale force.

1.3 Thrust Elemental Errors

In determining thrust uncertainty of a turbine engine, three major sets of elemental errors are dealt with. These errors deal with scale force (Table 1), inlet momentum (also known as ram drag), and area times delta pressure (across the engine) terms. Refer to Appendix B for a definition of these thrust terms. Elemental error sets for these terms establish the thrust uncertainty. This thesis will focus on reducing the elemental errors of scale force, as identified in Appendix B and defined in Table 1. Table 1 shows a spreadsheet of various bias and precision elemental errors associated with scale force measurement error sources with typical error values at certain scale force levels which are accounted for in an altitude simulating test cell. The critical scale force elemental errors are shown as item numbers 6, 13, and 16 in Table 1. These three elemental errors have been found to have the largest influence on scale force uncertainty in low thrust regions. These scale force elemental errors, along with the others shown, are combined to obtain the scale force uncertainty which is propagated into thrust uncertainty. The low scale force (thrust) region of an engine's operating envelope deserves special attention because

the critical scale force elemental errors (hysteresis and zero shifts i.e. item numbers 6, 13, and 16 of Table 1) become significant, while the other terms are negligible at low scale force levels.

Table 1 (Cont.). Scale Force Elemental Errors.

Error Source Item No.	3K lb_f B,lbf	3K lb_f S,lbf	10K lb_f B,lbf	10K lb_f S,lbf	50K lb_f B,lbf	50K lb_f S,lbf	Error Source Description
1.	1	-	5	-	25	-	Uncertainty determined by PMEL in Calibrator including traceability to NIST.
	2.5	-	10	-	50	-	Shift in load cell calibrations at PMEL pre to post program.
2.	-	-	-	-	-	-	The engine is aligned on the thrust stand with a transit to a tolerance of less than 0.5°.
3.	-	-	-	-	-	-	Load cells were calibrated with the same type adapters as used in installation.
4.	-	-	-	-	-	-	Non-repeatability due to labyrinth seal is included in items 7, 10, and 13.
5.	2	-	5	-	25	-	A centerline calibration is performed and a correction applied to the data load cell calibration.
6.	-	25	-	15	-	6	Error due to system hysteresis determined from repeat applied loads calibrations.
7.	-	1	-	2	-	10	Error due to system non-repeatability determined from repeat applied loads calibrations.
8.	-	-	-	-	-	-	Error due to system non-linearity determined from applied loads calibration, included in Item 16 curve fit error.
9.	-	-	-	-	-	-	Error due to pressure effects on load cell is reduced by determining correction factor at PMEL. Pressure measurement error is included in Item 10.
10.	1	3.6	1	3.6	1	3.6	Error due to the effect of pressure changes on the test cell, thrust stand, etc., as determined by vacuum check data.
11.	-	-	-	-	-	-	The service lines pressurization effects on tare are determined and corrections made to reduce this error to a negligible level.
12.	1	-	11	-	56	-	The load cell shift with temperature is

Table 1 (Cont.). Scale Force Elemental Errors.

Error Source Item No.	3K lb_f B,lbf	3K lb_f S,lbf	10K lb_f B,lbf	10K lb_f S,lbf	50K lb_f B,lbf	50K lb_f S,lbf	Error Source Description
							determined at PMEL.
13.	38	-	38	-	38	-	Zero shift including errors due to the effects of temperature on the thrust stand including errors induced through the test cell ground relative to the thrust stand are determined from pre and post test ambient data.
14.	-	-	-	-	-	-	The effect of vibration on the load cell is negligible and the effect on its output signal is reduced to a negligible level by applying a lowpass filter.
15.	1	1	2	5	10	25	Bias in the signal conditioning, shunt resistors, and A/D converter are calibrated to negligible levels prior to each test with the exception of the temperature effect on the calibrate load cell shunt cal. This bias error is reduced to ±0.02% by maintaining the ambient temperature on the cal load cell. System noise, resolution, and drift over the test period are accounted for in the ±0.05% precision.
16.	12	-	14	-	15	-	Curve fit error due to non-linearity of force measurement system.
17.	1	-	5	-	25	-	Data sampled and averaged for ten (10) seconds will reduce the sampling error to stated level assuming the instability does not exceed 1% of the average level and the frequency is not less than one hertz.

PART 2

ELEMENTAL ERROR REDUCTION

2.1 The Test Environment in an Altitude Simulating Test Cell

Air Force specifications are becoming more stringent, and for engine manufacturers to meet flight test requirements, thrust uncertainty resulting from altitude test facility measurements must be reduced. Thrust uncertainties of less than 1% are desired at critical "upper-left-hand" regions of the engine's flight envelope (Figure 1). In these low thrust areas (<10,000 lbf), scale force uncertainty accounts for over 90% of the total thrust uncertainty, while the remaining 10% relates to airflow and other measurement uncertainties. As a consequence, the elemental errors contributing to scale force uncertainty must be minimized. Through experiments and experience, the elemental errors associated with load cell hysteresis (Items 6 and 16 - Table 1) and thrust stand zero shifts (Item 13 - Table 1) have proven to be the primary contributors to scale force uncertainty and are the areas where control is to be emphasized. Thermal effects are also controllable factors, but cannot be quantified as an elemental error as such. However, thermal effects are contributing factors on many of the elemental errors dealt with and should be targeted for reduction. The previously introduced table, Table 1, lists the various elemental errors associated with scale force uncertainty and typical values at certain scale force levels, which are accounted for in an altitude simulating test cell. In the discussions and investigations to follow, all of the error source values in Table 1 will be assumed to hold constant, except those dealing with thrust stand hysteresis and zero shift (item numbers 6, 13 , and 16 of Table 1). Therefore, except for the errors 6, 13, and 16, the values of the remaining elemental errors in Table 1 will not be discussed.

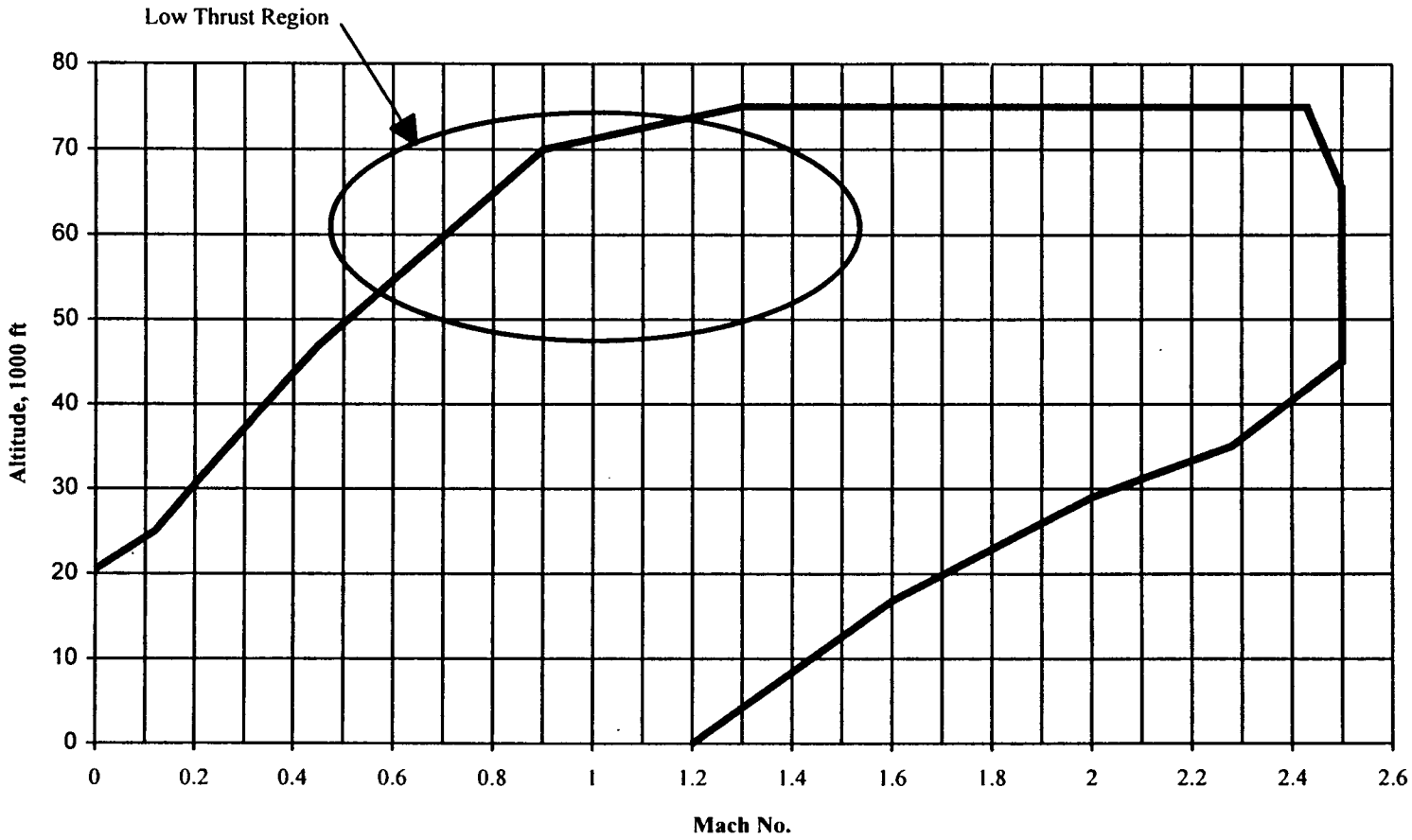


Figure 1. Typical Engine Flight Envelope

In the experiments evaluated in the present study, several factors need to be considered which may inhibit the use of this data in other test facilities. All of the experiments were performed in the C1 Altitude Test Facility at Arnold Engineering and Development Center, Arnold Air Force Base, Tullahoma, TN. Figures 2 and 3 display the typical configuration for the C1 Test Facility utilizing the scale force technique of thrust determination. The facility houses an overhead mounted floating thrust stand which is anchored to the rear bulkhead (also called the aft support rings) of the test cell by a the force measuring load train. The test cell is anchored to a concrete mass at the front end by a large I-beam. The thrust stand is rated for positive force measurements up to +50,000 lbf and negative force measurements to -30,000 lbf. Typically, turbine engines in the +30,000 lbf thrust class are tested in the cell. These cell characteristics are important when determining how applicable the results are to other facilities. While it may not be possible to apply the results directly to other facilities, the methods of reducing scale force uncertainty should certainly apply to other test facilities; that is, the techniques will apply and aid in reducing scale force uncertainty.

2.2 Effects on Scale Force Measurement

Many factors affect the accurate measurement of scale force. In order to achieve the lowest possible uncertainty, the contributions of such factors must be minimized. Hystersis, the contributions of thermal effects, and pre- to post-test load system zero shifts are the primary contributors to scale force uncertainty that will be targeted for

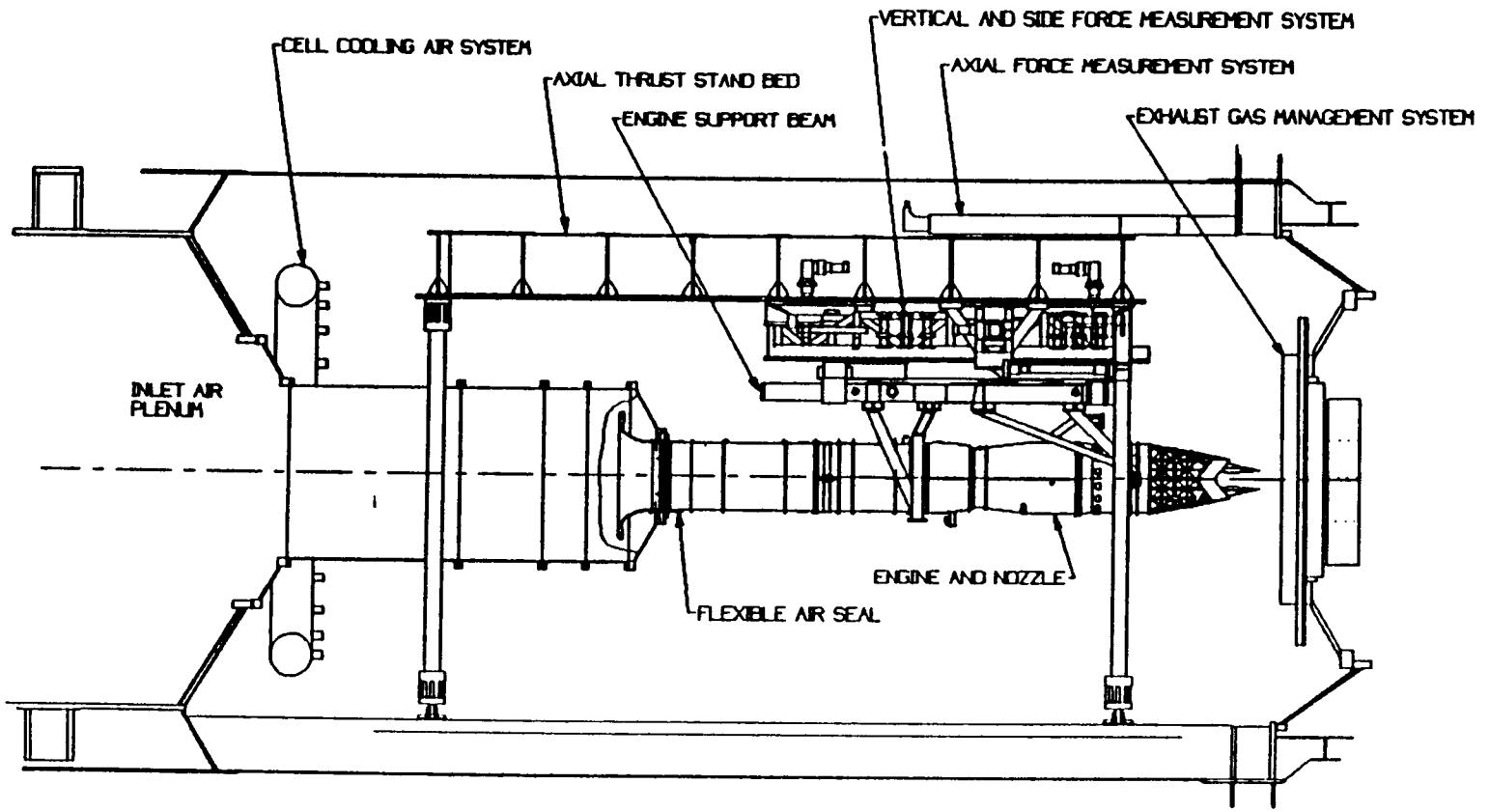


Figure 2. Turbine Engine Test Cell

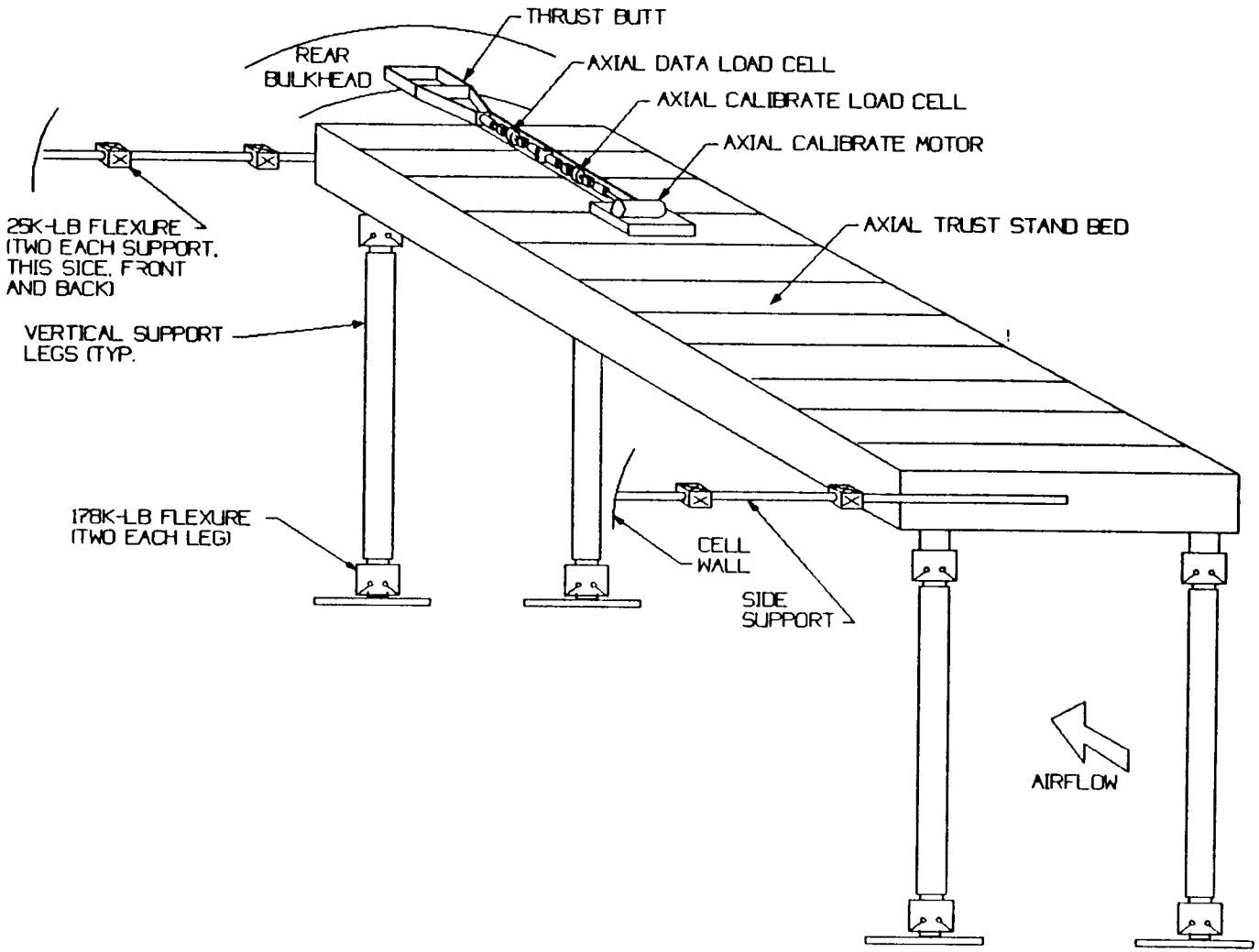


Figure 3. Turbine Engine Thrust Stand

reduction. In practice, these elemental errors have proven to directly impact the level of uncertainty achievable in low thrust flight regions of an engine's operating envelope.

2.2.1 Hysteresis Effects

As engine thrust levels decrease in the simulation of high altitude/low Mach Number flight regions, elemental errors which attribute to scale force uncertainty become very important. Thrust stand hysteresis is one such elemental error, which through calibration experiments, has been found to be reducible in the low thrust regions (0 lbf to +10,000 lbf). Hysteresis is defined as "the greatest difference between the measured output at equal applied forces when one output is obtained by increasing the force from zero to full scale and the other by decreasing from full scale to zero" [1]. This definition is also true when decreasing to negative full scale and returning to zero. A conventional type thrust stand calibration would include both positive full scale and negative full scale loading, the positive loading always being performed first. Appendix C identifies this type of calibration in Table C.1 "Conventional Thrust Stand Calibration."

In an ongoing effort to reduce thrust uncertainty at AEDC, several experiments were performed by the author to investigate the effect of calibration procedure on system hysteresis (which also leads to another elemental error: curve-fit errors - see Table 1). Hysteresis is found by plotting thrust stand tare versus the load being input to the thrust stand during a calibration procedure. Tare is defined as the difference between the load measured by the thrust stand measurement system and the load input to the thrust stand. The resulting tare curve would then be obtained in a normalized form through a second-

order curve fit. This curve fit is then applied, in the reduction of data obtained during a test period, to compute force corrections that add to or subtract from the load-cell measured engine force. The error in measured scale force due to hysteresis, from this process, (item numbers 6 and 16 of Table 1) should be evaluated and minimized to reduce scale force uncertainty and thus thrust uncertainty.

Three different experimental methods of thrust stand calibration were performed: 1) positive full scale (50,000 lbf) calibrations, 2) positive partial scale (10,000 lbf) calibrations, and 3) positive partial scale (+30,000 lbf) - negative partial scale (-10,000 lbf) calibrations. These experimental methods of thrust stand calibration will be evaluated in Part 3, versus a conventional style of thrust stand calibration wherein full scale positive to full scale negative calibrations are performed, to determine reductions in scale force uncertainty caused by reductions in the magnitude of hysteresis. Several changes in the characteristics of the tare curves were also noted in each of the experimental calibration procedures as will be identified in the remainder of this chapter.

2.2.1.1 Thrust Stand Calibration Experiments

A positive full scale calibration to 50,000 lbf was performed to determine if any reduction in the magnitude of hysteresis would occur, compared to a conventional calibration process (see Appendix C). It should be noted here that the targeted area for hysteresis reduction is at the 3,000 lbf level because this is the "low scale force level" being investigated. Data points were taken as identified in Appendix C, Table C.2 "50K Thrust-Side-Only Calibration." The comparison of this calibration with a conventional

calibration is shown in Figure 4. In this figure, the calibration process occurred in sequence: step 1, step 2, step 3, and step 4, as the direction arrows indicate. As can be seen in the figure, there is no change in hysteresis at 3,000 lbf load because the calibration points coincide with each other - the hysteresis being identified as the difference in tare values at a particular load. Based on this observation, no further analysis was done because no change or improvement was detected. However, a reduction in the curve-fit errors can be realized with this type of calibration versus the conventional calibration procedure. Appendix D displays how a curve-fit error is directly related to the level of hysteresis in the tare curve. This curve fit error reduction is due to the non-linearity of the tare curve when passing from positive to negative through zero load in the conventional thrust calibration. The non-linearity is a function of installation and other test cell-specific effects. Although this benefit is small compared to the hysteresis error, it is an important finding because any reduction of an elemental error will reduce scale force uncertainty. One point should be made about Figure 4 (and also to Figure 5 and Figure 6 which will be presented next) concerning the process for evaluating the hysteresis error. Figure 4 displays the results of two individual calibrations for comparison. The hysteresis error to be included in an actual scale force uncertainty analysis would be found by evaluating all calibration plots, using the selected calibration procedure, from a test program (typically 30 test periods resulting in 30 calibration plots). The hysteresis error would then be defined as the maximum value of hysteresis found in

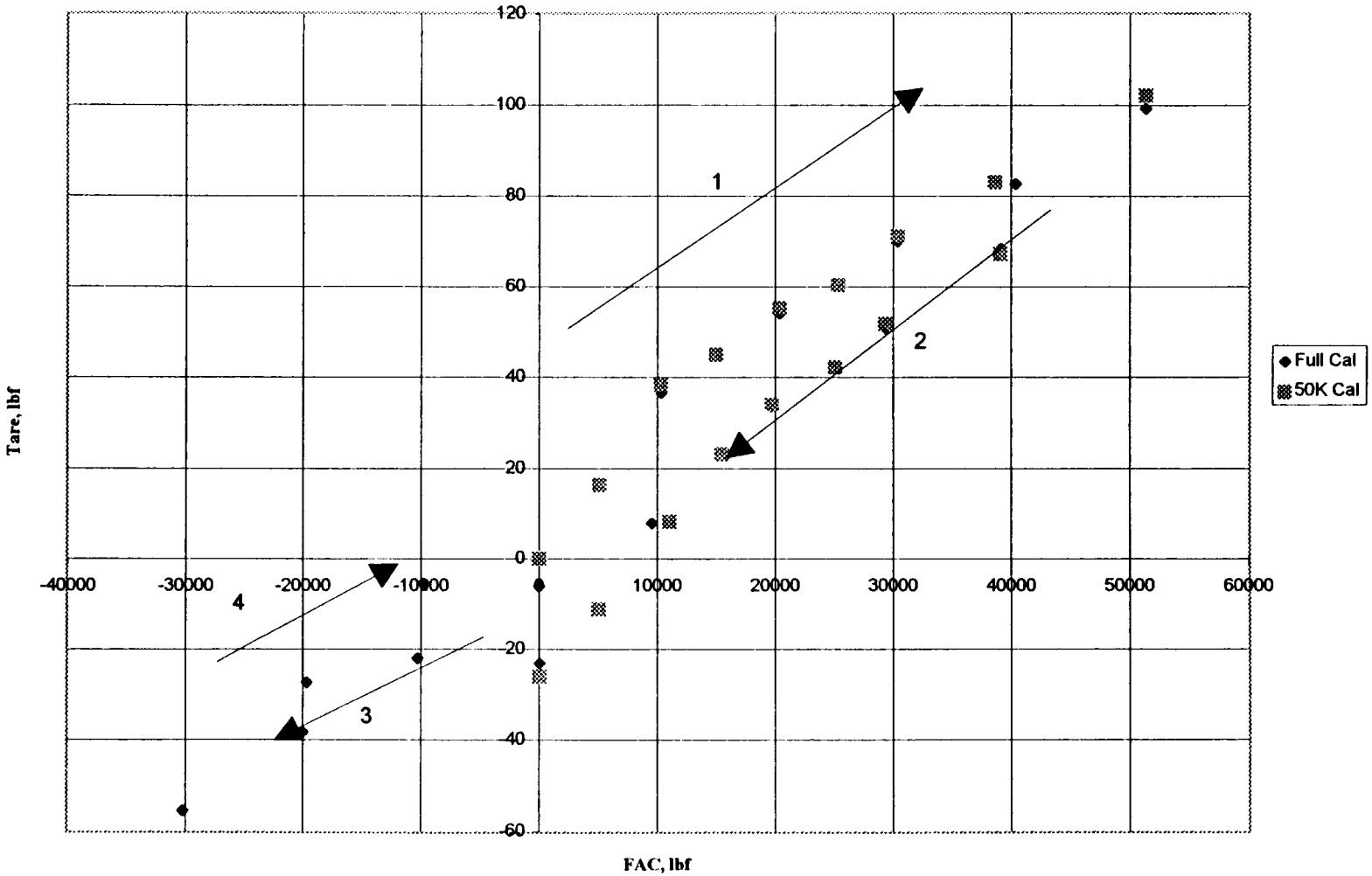


Figure 4. Positive 50K Cal vs Conventional Cal.

these plots at the scale force level where uncertainty is desired to be calculated - which is 3,000 lbf for this discussion.

A positive partial scale calibration to 10,000 lbf was next performed for analysis. The results are reviewed under Analysis 2 of Part 3. Data points were obtained as identified in Appendix C, Table C.3 "10K Thrust-Side-Only Calibration." As seen in Figure 5, a major and significant reduction of hysteresis at 3,000 lbf was attained. This is due to a thrust stand characteristic which has been called "thrust stand toggle" (Figure 5). Toggle is directly influenced by the magnitude of force imparted to the thrust stand during calibration and/or testing. For example, if the thrust stand is flexed to 10,000 lbf and returned to 0 lbf, there will be less hysteresis versus when the stand is flexed to 50,000 lbf and returned to 0 lbf, hence smaller toggle. This can be seen in Figure 4 and Figure 5 when comparing the 10,000 lbf and 50,000 lbf "Thrust-Side-Only" calibrations. The resulting hysteresis will be further reduced if the thrust stand is also flexed with a negative load, i.e. moved in the negative direction. To explain this more clearly, consider the following scenario. When the thrust stand is flexed to a positive 50,000 lbf load and returned to zero, the absolute value of hysteresis will be approximately 23 lbf (a change in zero readings from 0 lbf to -23 lbf). Remember the definition of hysteresis - see Glossary of Terms. If the thrust stand is then flexed to a negative value, say -10,000 lbf and returned to 0 lbf, the zero reading will be about -5 lbf. Thus, a toggle type movement is being realized. This is a result of test cell-specific/installation effects. This toggle is very important and its control will be instrumental in reducing scale force uncertainty

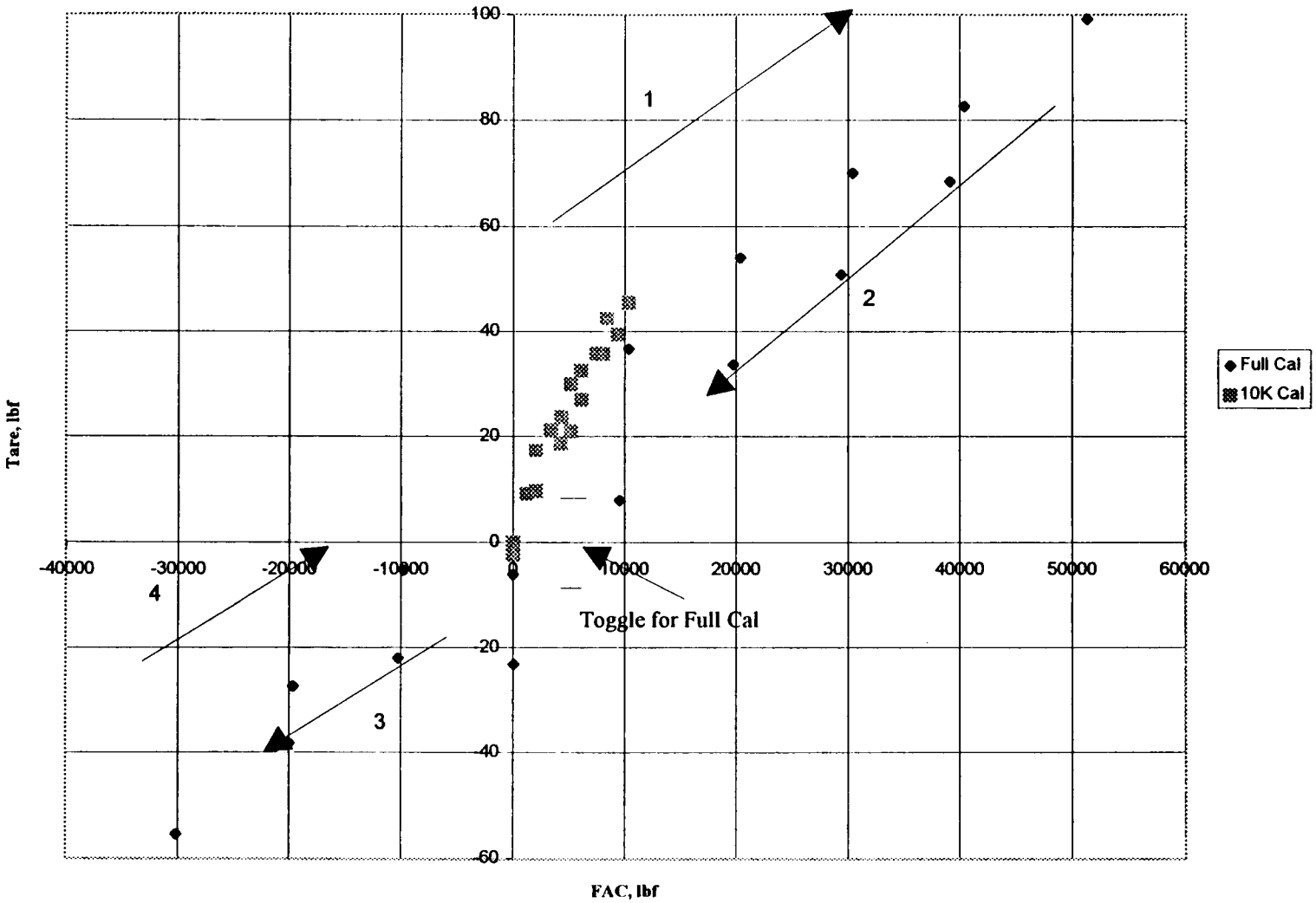


Figure 5. 10K Cal vs Conventional Cal.

levels. One further improvement to be noted here is that curve-fit error is reduced. This error would be realized when comparing the average of the up and down tare values with a second order curve-fit through all data points. It is minimal here because the tare curve is much more compact for the +10,000 lbf calibration when comparing to the positive full scale calibration or the conventional method of calibration.

A final experiment of a positive partial scale force (30,000 lbf) to a negative partial scale force (-10,000) calibration was performed to evaluate the possibility of having more flexibility in the flight envelope during a test period. See Figure 6 for the results of this experiment. This data is evaluated in Analysis 5 of Part 3. The procedure for this calibration is identified in Appendix C, Table C.4 "+30K to -10K Thrust Calibration." As can be seen from Figure 6, there is some reduction in hysteresis (and therefore curve fit error) at the 3,000 lbf level. Although the benefit is somewhat less than the 10K Thrust-Side-Only Calibration, there is more benefit than the 50K Thrust-Side-Only Calibration and the Conventional Thrust Stand Calibration. This fact is important when deciding which thrust stand calibration procedure to follow for a test period of a given engine test program. The trade off for the lowest uncertainty is the limit of flight conditions that can be processed with any particular calibration sequence; however, slightly higher uncertainties may be acceptable with another type of calibration to gain flexibility for testing in the engine's flight envelope. During a typical test period, the thrust stand will encounter positive thrust loads from an engine above 10,000 lbf and negative drag loads below 0 lbf. For this reason, it is important to determine thrust stand

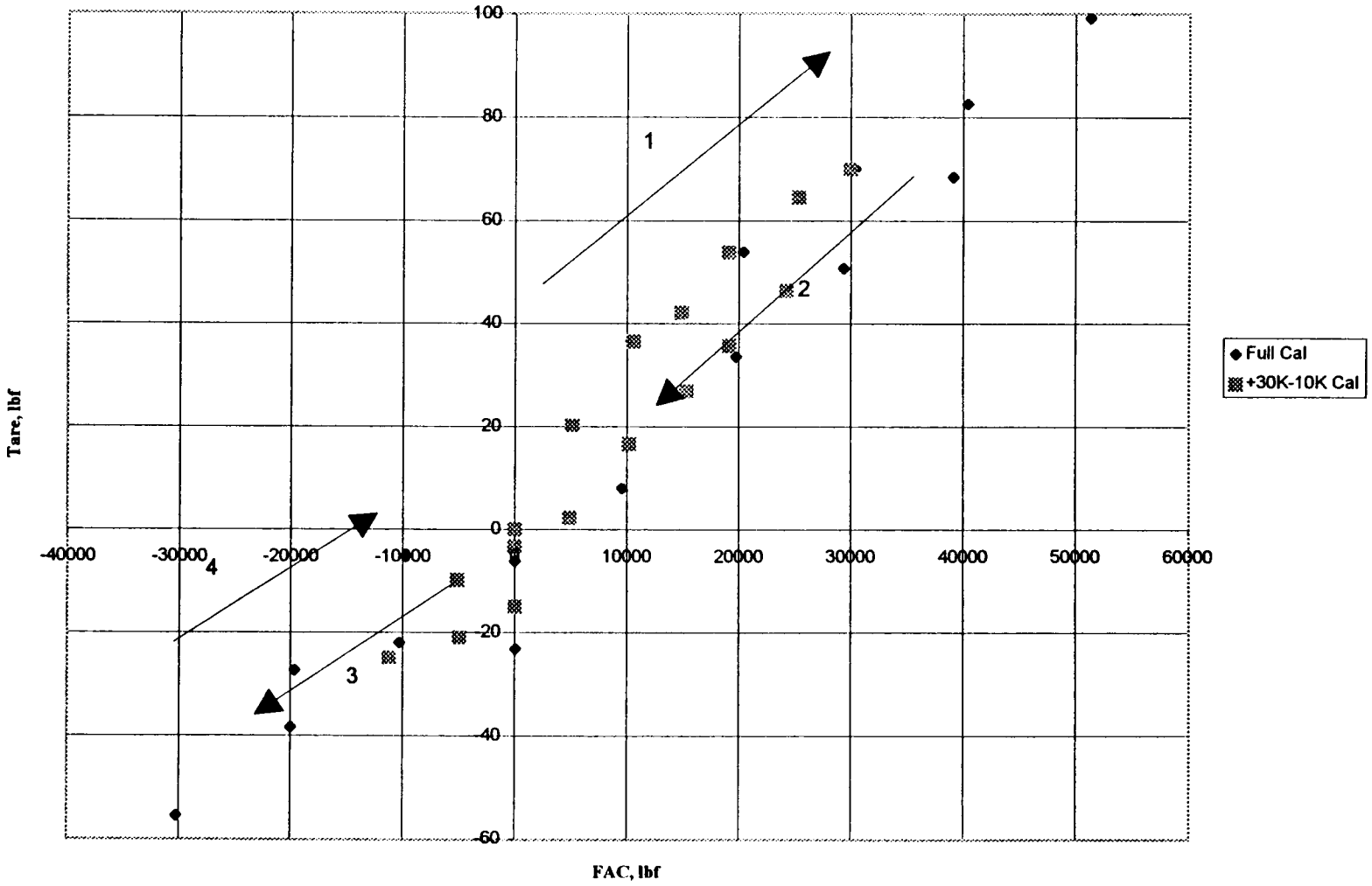


Figure 6. +30K/-10K Cal vs Conventional Cal.

characteristics for the type of test being conducted to minimize the level of thrust uncertainty for that type of test. This will allow for more flexibility, as far as test objectives are concerned, during a test period.

In general, when the thrust stand was flexed to +10,000 lbf and returned to 0 lbf, the tare curve had significantly lower hysteresis versus when the stand was flexed to +50,000 lbf and returned to zero or when the stand was flexed to full scale positive and negative values. The 10K and 50K positive type experiments revealed less non-linearity of the tare curve, when compared to the conventional calibration, which affects items 6 and 16 of Table 1. However, in performing the experiments, the benefit of flexing (or calibrating) the stand to reduced calibration load values was seen to diminish as calibration loads approach +15,000 lbf to +20,000 lbf. Thus, the greater the thrust stand is flexed by higher calibration loads, the more the load system hysteresis will be. As can be seen from Figures 4 and 5, the hysteresis at 3,000 lbf is approximately 25 lbf for a +50,000 lbf calibration whereas it is negligible for +10,000 lbf calibration.

In summary, therefore, when performing a test in a low thrust region, the thrust stand can be calibrated with a reduced loading level, resulting in lower hysteresis levels and therefore a lower scale force uncertainty.

2.2.2 Thermal Effects

Minimizing thermal effects is another major area of promise in reducing scale force uncertainty at low thrust levels. Severe in-cell temperature conditions encountered during test operations are quite common and steps must be taken to ensure good

measurements. Unfortunately, thermal growth of the test cell, temperature effects on the thrust stand, and other thermal effects are not accounted for in a scale force uncertainty analysis. However, these thermal effects have far reaching implications on many of the elemental errors considered in such an analysis. For this reason, thermal effects must be discussed as well as methods of reducing them.

Test cells and thrust stands are primarily constructed of steel. Typical configurations have been shown in Figure 2 and in Figure 3. The aft end of a test cell typically reaches temperatures up to 200 °F during a test, due to heating by engine exhaust, while the front end of the cell remains near ambient temperatures due to injected secondary cooling air. Thermal growth and/or distortion of the steel cell walls results. This growth is detrimental to scale force readings. The force measuring data load cells are located in and attached to the aft region of the cell and are subjected to a severe temperature environment. This causes errors to arise due to load cell heating (temperature effects on the strain gages). Another reason that test cell temperature gradients should be avoided is due to the fact that numerous (~1000) service lines connect the thrust stand to the grounded cell structure. These connections are referred to as line flexures and are designed to allow minimum interference with the floating stand. The cell heating causes non-uniform growth of the flexures with respect to ground and imparts unwanted force on the load cells, via the connection with the thrust stand. These effects cannot be avoided; however, it is imperative that they be minimized.

Minimizing load cell heating effects can be accomplished in several ways. Maintaining the temperature of the load cell to within +/- 10 °F of the value during calibration of the thrust stand, at the start of the test, is very important. This can be done by using maximum amounts of test cell cooling airflow between performance data points. This cooling air is drawn into the test cell, from the atmosphere, due to the difference in ambient and cell pressures when at an altitude flight condition. Also, check and, if necessary, reroute service lines to ensure that minimum forces are exerted on the floating stand. This will minimize service line thermal growth problems that could impart a force in the axial direction. For example, fuel supply lines, electrical connections, and so forth, should attach to the thrust stand orthogonal to the line of thrust. Flexures oriented in line with thrust will directly affect axial scale force measurement if thermal growth occurs. In evaluating the C1 service line flexures, three 4" diameter stainless steel pipes were identified as being incorrectly routed onto the thrust stand. This discovery proved to be very instrumental in reducing zero shifts (see Figure 7 in the Zero Shift section to follow). Other recommendations will be discussed later.

Thermal effects can also be introduced in other ways. Altitude simulating test cells, such as the C1 Test Facility at AEDC where the experiments were performed, are basically of a cylindrical tube design. The test cells are anchored at the front to a very large concrete mass. The aft end of the cell is allowed to thermally grow to the rear toward the exhaust ducting. Because of the extreme mass of steel in the cell structure, along with the fact that hatches and ports disrupt the continuity of the cylinder (cell),

irregular growth of the cell results. This type of growth, which can also be magnified by the difference in cell and ambient pressures, will be referred to as an "oil can effect." With this in mind, remember from previous discussion that the thrust stand is anchored to the cell at the aft end where significant thermal expansion and contraction occurs. This growth provides an avenue to impart unwanted forces to the floating stand, which is another reason to relocate the load cells to the front of the test cell. In the C1 Test Facility, a delta growth between the north and south sides of the aft end of the cell have been observed to be as large as 0.015 inches. This can be a significant problem for force measurement due to the fact that the travel of the thrust stand is 0.0015 for 1000 lbf of applied load. This unwanted cell movement can be minimized by requiring that certain temperature limits are followed, as will be discussed in the Recommendations section of this paper.

2.2.3 Zero Shift Effects

Pre- to post-test zero shifts are an elemental error of scale force/thrust uncertainty which is easily controlled if operating procedures to contain them are followed. Zero shifts are primarily related to thermal effects. A zero shift is defined simply as the difference in zero readings of the data load cells taken at different times, primarily before and after a test period. Before a test begins, the thrust stand is flexed (see Appendix C Table C.1 for procedure) to positive full scale value then to negative full scale value and returned to zero. A data point is then recorded to obtain the load cell readings as a zero load reference point. The test is then conducted, and the same procedure is used post-test

to determine the shift in zero load reference points. The difference between the zero load readings is called the pre- to post-test zero shift, and is used to estimate measurement errors or to adjust the data for that test period. Appendix E graphically displays the zero shift error. Depending on the severity of test cell environmental conditions, this value can be significant especially in the low scale force (hence low thrust) regions of the flight envelope.

The major contributors affecting zero shifts are thermal effects on the test cell and data system. In the C1 Test Facility, there are approximately 1,000 individual service line flexures connecting the thrust stand to ground. These service line flexures are made up of such necessities as fuel piping, raw water piping, and pressure sensing lines. As temperature gradients in the cell increase, non-uniform thermal growth results in the flexures. The thermal growth will cause the flexures to impart unwanted forces onto the thrust stand that previously were unaccounted for in the pre-test data. Also due to the temperature gradients, non-uniform growth of the test cell structure will result. From Figures 2 and 3, it can be seen how the thrust stand is attached to the cell structure (i.e. through the axial force measurement system to the rear bulkhead). These factors were discussed in the Thermal Effects section of this chapter. Appendix F presents an analysis which shows how the reduction of thermal gradients in the cell directly affects zero shifts. By understanding the installation of the thrust stand and the exposure of service lines to severe conditions experienced during a test, the importance of correctly routing flexures onto the thrust stand becomes vital. As previously stated, the re-routing of several service

line flexures in C1 helped in reducing the zero shifts as can be seen from the trends of the data shown in Figure 7. Figure 7 shows the improvements in zero shifts by combining the previously stated findings. This information was accumulated from actual test data and has aided in reducing scale force uncertainty to lower levels. As seen in Figure 7, reduced zero shifts realized average about -20 lbf. This average was reduced down from an averaged value of about -70 lbf, before service lines were rerouted, and -35 lbf, with rerouted service lines and some temperature limits as identified on Figure 7. In Part 4, the value of -20 lbf, for zero shifts, will be used for Analyses 3 through 5 to help obtain realistic goals for scale force uncertainty reduction.

2.2.4 Data System Effects

The data acquisition system and its components are also susceptible to the severe test conditions. As seen in Figure 2, the force measurement system is located in the rear of the test cell where the exhaust plume of the engine is captured by the diffuser. The temperatures of the cell structure in this aft region frequently reach 150°F to 200°F. This high temperature environment can have an adverse affect on the data load cells used to measure scale force. Although the load cells are constructed to minimize and can be calibrated to identify temperature effects, repeated exposure of electronic equipment to high temperatures has an adverse and sometimes unknown effect. To ensure credible scale force measurements, the load cells and other electronic equipment must be protected from the high temperatures. Another factor affecting zero shifts which stem from the electronic equipment is "data system drift." Prior to any engine test, the data system is

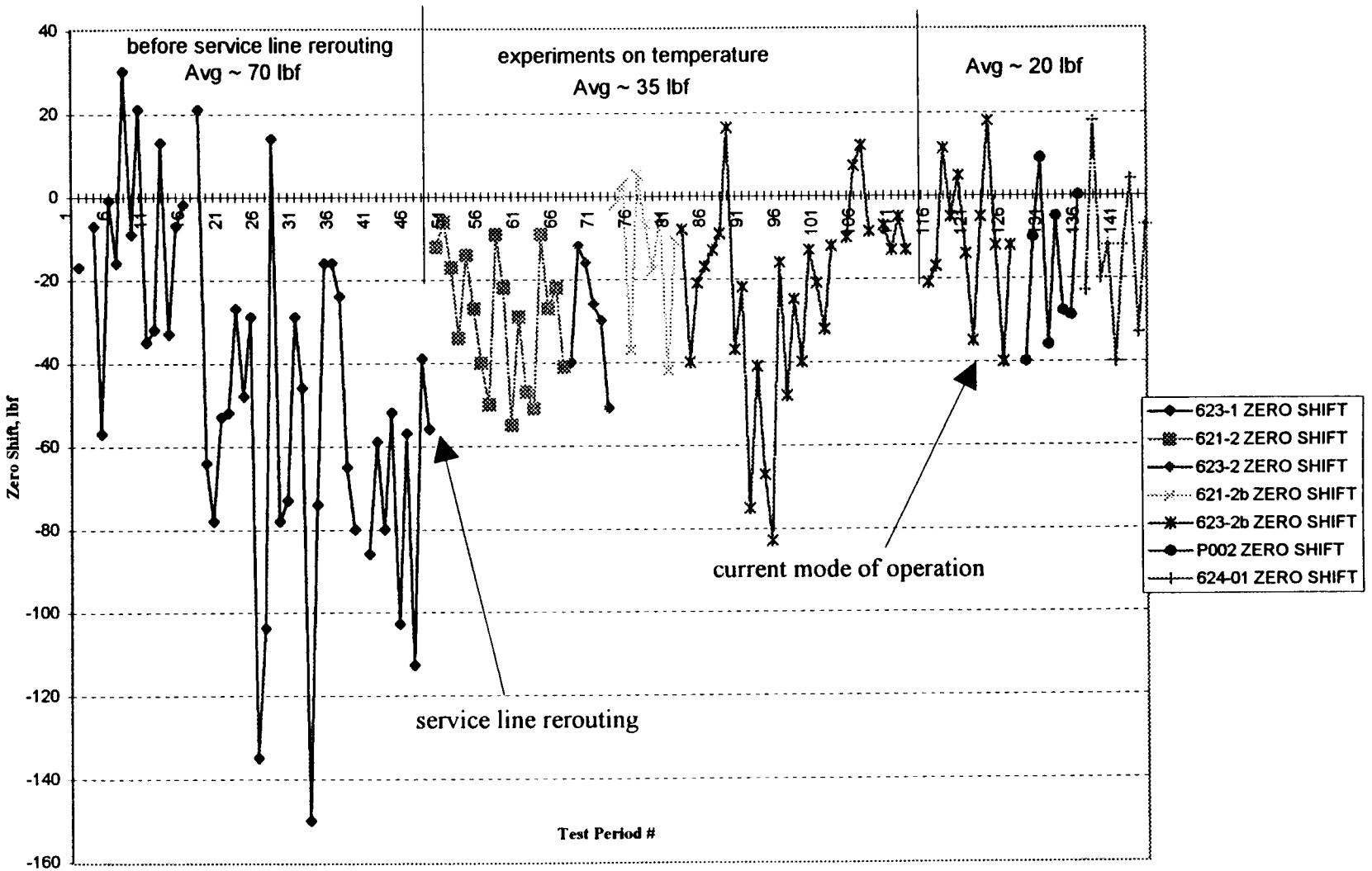


Figure 7. Zero Shift History

calibrated while instrumentation is surrounded by an environment at some ambient condition. Typically, an engine test will be 10 to 18 hours in duration; however, some tests can last as long as 40 hours or more depending on objectives. Over the course of a day or several days, that is extended periods between calibrations, different environmental ambient conditions arise. The effect of time and changing environmental conditions on data system recording is termed "data system drift." Mainly, this drift is attributable to environment effects on pressure transducers, thermocouple systems, and so forth, not to changes in the microprocessor and computer based data recording and processing equipment. Although the changes in ambient readings may be minimal, the compounding effect of the high temperature environment of the test cell can make the error significant. Suggestions for containing these effects will be made in Part 4.

2.3 Future Work

Through several experiments to determine characteristics of stand/load cell hysteresis, a possible way to further minimize zero shifts was determined. It should be mentioned before discussion that this characteristic is not fully understood. As previously mentioned, it was found that when the stand was flexed to a lower scale force value, the thrust stand hysteresis decreased. Although further experiments must be performed, this finding suggests that the zero reading obtained pre-test will be affected by the level of scale force achieved during testing. The possible benefits of this finding will be explained as it pertains to the conventional calibration. The difference in zero readings

can be off-set by flexing the stand to an intermediate level (+15,000 lbf) after the pre- and post-test flexes. This intermediate flex places the zero reading at a value associated with the level of scale force achieved in any region of the flight envelope. Refer back to the Hysteresis Section of this chapter for the tare curve characteristics. Therefore, the zero reading will remain the same unless the engine thrust rises above the intermediate flex value (+15,000 lbf). To explain this, consider the following. Suppose the thrust stand is to be calibrated from +50,000 lbf to -30,000 lbf. The hysteresis at zero load will thus be approximately 25 lbf. The pre-test zero reading (for data reduction) would be acquired here which is at the top of the hysteresis band. If the test was then conducted, and engine thrust levels reached +50,000 lbf, the zero reading would be -25 lbf as obtained in the calibration. A post-test flex would then be conducted in the same manner as the pre-test flex, the only difference being that there is now a new starting point or zero point for the procedure. Ideally, the original zero reading of the pre-test load procedure should be used for data reduction. However, in the post-test load procedure, there is a new starting point which will have a negative impact and cause a zero shift. Note that the purpose of the pre- and post-test flex procedures is not only to obtain an averaged zero reading for data reduction purposes but also to ensure that the thrust stand is able to translate freely. This zero shift may also be compounded by thermal effects during the test, as discussed previously. To minimize this shift for scale force uncertainty reduction purposes, performing a flex to +15,000 lbf and returning to zero load after the pre- and post-test flex procedures will place the "true" zero in the middle of the hysteresis band. If the

same test scenario were again repeated, the shift would now be approximately half the original value. Higher intermediate flex values are of little use because the benefit disappears when loadings are greater than approximately +20,000 lbf. The benefit disappeared because above +20,000 lbf, the full hysteresis band at zero load is realized. Once again, this phenomenon is not fully understood. Further experiments should be performed on the load cells at high force levels to determine the extent of this effect. Some zero shifts cannot be avoided due to the fact that drag conditions and thrust levels above +15,000 lbf may be experienced during a test. However, these effects are minimal contributors to uncertainty at high scale force conditions.

PART 3

METHODS AND ANALYTICAL RESULTS

3.1 Analysis Methodology

The ultimate objective of this thesis is to evaluate the effects of reduced elemental errors on scale force uncertainty. To this point in the discussion, the primary elemental errors (hysteresis, zero shift, and the contributions of thermal effects) have been investigated. In reviewing the analytical results to follow, an important factor must be considered. It is desired to obtain the lowest scale force uncertainty levels possible in the area of low scale force (thrust). As previously identified, a scale force reading of 3,000 lbf typifies engine scale force levels in the upper-left-hand region of typical military engine flight envelopes. In selecting procedures to achieve low uncertainty at 3,000 lbf, flexibility in achieving test objectives is very important to keep test efficiency high. Therefore, final selection of a procedure must account for this fact, even if a trade-off in higher uncertainty levels must be accepted. The results of analyzing the calibration procedures for the load measuring system will be presented in order from highest resulting uncertainty to lowest uncertainty, as identified by the root-sum-square methodology.

The uncertainty analysis methodology compares the results of five calculations of scale force uncertainty which include the estimated effects from the earlier findings, namely the Hysteresis Effects, Thermal Effects, and Zero Shift Effects sections of Part 2. From these earlier findings, lower hysteresis values were shown to result from the type of calibration procedure used. Zero shift reductions were realized by following temperature

restrictions to reduce in-cell thermal gradients and by proper routing of service lines to the engine. The elemental uncertainty reductions of the thrust measuring system, with and without modified calibration procedures, will be applied in this section of the thesis to assess their impact on overall scale force measurement uncertainty.

To explain the format for all of the analyses, refer to Table 2. There are two sets of data in the table. The left-hand group contains information used to determine the bias error for this analysis. The first column in this group identifies the elemental error item number displayed in Table 1. This reference will aid in identifying a particular error. The second column in this group is the value, in lbf, determined for the elemental error identified in the first column. This elemental error value was derived as explained in Table 1. The third column is the elemental error value squared. Because the root-sum-square method of uncertainty determination is to be used, the sum of the elemental error values squared is needed. The fourth column identifies this sum. The fifth column displays the square root of the sum of the elemental error values squared. The right-hand group of data contains information used to determine the precision error for the analysis. The precision error group is structured identically to the bias error group. The uncertainty values, determined from the bias and precision values shown in column five of each of the respective groups, will be displayed in the Analysis Summary in Table 7. The Analysis Summary table will display the bias and precision error values in lbf, the additive and root-sum-square uncertainty values in lbf and percent of 3,000 lbf for all five calculations.

Table 2. Results of Analysis 1 of Elemental Errors on Scale Force Uncertainty.

Note: Application to 3,000 lbf Scale Force Measurement: Full Conventional Calibration without Reduction in Hysteresis or Zero Shift.

3K lbf Bias error

Table 1 item #	values, lbf	squares	sum of squares	sqrt of sum of squares, lbf
1a	1	1	1626.2644	40.32696864
1b	2.5	6.25		
2		0		
3		0		
4		0		
5	5	25		
6		0		
7		0		
8		0		
9		0		
10	0.12	0.0144		
11		0		
12	1	1		
13	38	1444		
14		0		
15	2	4		
16	12	144		
17	1	1		

3K lbf Precision error

Table 1 item #	values, lbf	squares	sum of squares	sqrt of sum of squares, lbf
1a		0	895.6936	29.9281406
1b		0		
2		0		
3		0		
4		0		
5		0		
6	25	625		
7	2	4		
8		0		
9		0		
10	0.06	0.0036		
11		0		
12		0		
13	16.3	265.69		
14		0		
15	1	1		
16		0		
17		0		

U = [(40.327)^2 + (2(29.928))^2]^.5 = 72.17 lbf

3.2 Scale Force Uncertainty Analysis

3.2.1 Analysis 1

Analysis 1 will be used as the baseline analysis because it includes no reductions in hysteresis or zero shifts. For this analysis, a conventional thrust stand calibration procedure (Appendix C Table C.1) was performed. This is the nominal mode of operation in the C1 Test Facility. As shown earlier, the hysteresis for such a calibration will have the maximum value when compared to other types of calibration procedures. This analysis also uses zero shift data from a previous test program for which there was no attempt to reduce zero shifts. Although techniques for obtaining zero shift reductions have been realized (see Figure 7) in subsequent test programs, this baseline analysis will not reflect these numbers.

The elemental error values for Analysis 1 are shown in Table 2. In viewing the table, it is seen that some of the elemental errors have a value of zero. This is due to the fact that this format is used to "book-keep" all elemental errors to avoid the re-application of errors in the thrust uncertainty calculation, whereas in the present study, only scale force uncertainty calculations are being performed. The remaining values in the table will remain constant, except for the two bias error terms and two precision error terms for hysteresis and zero shift, in an effort to identify the contributions of these two critical elemental errors on overall scale force measurement uncertainty. The two variable bias error terms in the analysis are item numbers 13 and 16 (see Table 1 for description). Bias error term 13 is the average all of zero shifts obtained in a test program. Bias error term

16 encompasses the error of curve-fitting the non-linear hysteresis data (Appendix D). The two variable precision error terms are item numbers 6 and 13. Precision error 6 is obtained from the maximum value of system hysteresis determined from the thrust calibrations performed over a test program. Precision error 13 is the standard deviation of the zero shift data. The hysteresis related errors (bias error 16 and precision error 6) were obtained from the full conventional calibration, the results of which are shown in Figure 4. The zero shift related errors (bias error 13 and precision error 13) were obtained from an actual test program, performed in the C1 Test Facility, in which no attempt was made at reducing zero shifts. The uncertainty obtained from Analysis 1 for scale force measurement due only to thrust stand loading hysteresis and load cell zero shift was 72.17 lbf or 2.41 % of 3,000 lbf.

The remaining analyses will follow the same methodology. The hysteresis values will reflect the results of the various calibrations evaluated in the Hysteresis Effects section of Part 2. The zero shift values will reflect values of previously obtained data from several test programs. The different zero shift values to be presented are data from tests where the zero shift reduction methods were employed, as well as data obtained from tests without zero shift reduction methods employed.

3.2.2 Analysis 2

Analysis 2 was the first attempt to evaluate a reduction in scale force uncertainty for low thrust tests. In contrast to Analysis 1, a positive 10,000 lbf calibration was performed. This procedure was defined earlier and is identified in Appendix C, Table

C.3 "10K Thrust-Side-Only Calibration." Figure 5 (Part 2) showed the plotted results of this calibration versus the full conventional calibration of Analysis 1. Several improvements should be noted here. First, there is a drastic reduction in hysteresis throughout the calibration range. Next, the non-linear region near zero applied load that occurs in the full calibration, when passing from positive to negative loading, is avoided. This calibration improvement significantly reduces the hysteresis related errors. The data shown in Table 3 reflects these improvements. Item number 6 of the precision errors has been reduced from 25 lbf, in Analysis 1, to 2.5 lbf. In relation to zero shift, no changes were made because the same zero shifts were used as in Analysis 1 (i.e. the zero shift values with no attempt at reduction). Therefore, this analysis shows the improvement in uncertainty related only to hysteresis. As shown in Table 7, which is the summary of analytical uncertainties, the root-sum-square uncertainty of scale force is now 51 lbf or 1.7 % of 3,000 lbf.

3.2.3 Analysis 3

Analysis 3 was evaluated with a full conventional calibration to identify improvements attainable if zero shifts are reduced to -20 lbf. As previously discussed, C1 zero shifts can be reduced to this level when modifications are made to operating temperature limits, and properly routed thrust stand and engine service lines (as identified in the Thermal Effects and Zero Shift sections of Part 2) are installed. Therefore, in contrast to Analysis 2, the full conventional calibration hysteresis values and the reduced zero shift values that were obtained are shown in the uncertainty table (Table 4). The

Table 3. Results of Analysis 2 of Reduced Elemental Errors on Scale Force Uncertainty.

Note: Application to the 3,000 lbf Scale Force Measurement: 10K Thrust-Side-Only Calibration with Reduced Hysteresis but Full Zero Shift Effects.

3K lbf Bias error

Table 1 item #	values, lbf	squares	sum of squares	sqrt of sum of squares, lbf
1a	1	1	1491.2644	38.61689268
1b	2.5	6.25		
2		0		
3		0		
4		0		
5	5	25		
6		0		
7		0		
8		0		
9		0		
10	0.12	0.0144		
11		0		
12	1	1		
13	38	1444		
14		0		
15	2	4		
16	3	9		
17	1	1		

3K lbf Precision error

Table 1 item #	values, lbf	squares	sum of squares	sqrt of sum of squares, lbf
1a		0	276.9436	16.64162252
1b		0		
2		0		
3		0		
4		0		
5		0		
6	2.5	6.25		
7	2	4		
8		0		
9		0		
10	0.06	0.0036		
11		0		
12		0		
13	16.3	265.69		
14		0		
15	1	1		
16		0		
17		0		

U = [(38.617)^2 + (2(16.641))^2]^.5 = 50.9 lbf

Table 4. Results of Analysis 3 of Reduced Elemental Errors on Scale Force Uncertainty.

Note: Application to the 3,000 lbf Scale Force Measurement: Full Conventioanal Calibration with Full Hysteresis but Reduced Zero Shifts.

3K lbf Bias error

Table 1 item #	values, lbf	squares	sum of squares	sqrt of sum of squares, lbf
1a	1	1	582.2644	24.13015541
1b	2.5	6.25		
2		0		
3		0		
4		0		
5	5	25		
6		0		
7		0		
8		0		
9		0		
10	0.12	0.0144		
11		0		
12	1	1		
13	20	400		
14		0		
15	2	4		
16	12	144		
17	1	1		

3K lbf Precision error

Table 1 item #	values, lbf	squares	sum of squares	sqrt of sum of squares, lbf
1a		0	630.0036	25.09987251
1b		0		
2		0		
3		0		
4		0		
5		0		
6	25	625		
7	2	4		
8		0		
9		0		
10	0.06	0.0036		
11		0		
12		0		
13	0	0		
14		0		
15	1	1		
16		0		
17		0		

U = [(24.13)^2 + (2(25.1))^2]^.5 = 55.69 lbf

data in Table 4 shows significant changes with respect to the baseline analysis of Analysis 1. The changes result in the values of item number 13 of the bias errors and item number 13 of the precision errors. The new values are now 20 lbf for bias error 13 and 0 lbf for precision error 13. The resulting scale force uncertainty for this Analysis 3 (see Table 7) was significantly reduced to 55.7 lbf or 1.86 % of 3,000 lbf. Thus, it is apparent that reducing the zero shift elemental error has the same relative impact on scale force measurement uncertainty as hysteresis reduction, for the C1 load measuring system.

To this point in the analysis, the individual effects of those elemental errors denoted hysteresis and zero shifts have been identified. As anticipated, both of these types of elemental errors make contributions to scale force uncertainty in the low scale force regions of an engine's flight envelope.

3.2.4 Analysis 4

Analysis 4 was performed to quantify the combined effects of hysteresis and zero shift reductions on scale force uncertainty. The reduced hysteresis values used in Analysis 2 and the reduced zero shift values used in Analysis 3 were inserted into Table 5 for this analysis. The Analysis Summary (Table 7) shows that the resulting 22.2 lbf (.74 % of 3,000 lbf) scale force uncertainty is the lowest value attainable for the combined reductions. As previously identified in Analyses 2 and 3, the hysteresis reductions resulted in bias error 16 having a value of 3 lbf and precision error 6 having a value of 2.5 lbf. Also, the zero shift reductions resulted in bias error 13 having a value of 20 lbf and precision error 13 having a value of 0 lbf. This analysis forms the basis for identifying a

Table 5. Results of Analysis 4 of Reduced Elemental Errors on Scale Force Uncertainty.

Note: Application to the 3,000 lbf Scale Force Measurement: 10 K Thrust-Side-Only Calibration with Reduced Hysteresis and Reduced Zero Shifts.

3K lbf Bias error

Table 1 item #	values, lbf	squares	sum of squares	sqrt of sum of squares, lbf
1a	1	1	447.2644	21.14862643
1b	2.5	6.25		
2		0		
3		0		
4		0		
5	5	25		
6		0		
7		0		
8		0		
9		0		
10	0.12	0.0144		
11		0		
12	1	1		
13	20	400		
14		0		
15	2	4		
16	3	9		
17	1	1		

3K lbf Precision error

Table 1 item #	values, lbf	squares	sum of squares	sqrt of sum of squares, lbf
1a		0	11.2536	3.35463858
1b		0		
2		0		
3		0		
4		0		
5		0		
6	2.5	6.25		
7	2	4		
8		0		
9		0		
10	0.06	0.0036		
11		0		
12		0		
13	0	0		
14		0		
15	1	1		
16		0		
17		0		

$U = [(21.14)^2 + (2(3.35))^2]^{.5} = 22.2$ lbf

possible new procedure for performing thrust stand calibrations, when testing turbine engines in low scale force regions. One drawback of this reduced uncertainty calibration procedure is that by calibrating the thrust stand to 10,000 lbf , the test period cannot include test points with higher engine thrust, i.e. other areas of an engines flight envelope. This may be a prohibitive drawback in some test programs because, since testing is expensive, it is usually not practical to limit test objectives to include only the low scale force regions of the flight envelope.

3.2.5 Analysis 5

Analysis 5 was performed to investigate the possibility of performing a partial scale (+30K lbf to -10K lbf) calibration, while maintaining low zero shifts, and achieving low scale force uncertainty. Analysis 4 showed that low scale force uncertainty can be realized with combined methods of reducing hysteresis and zero shifts. A trade-off to this low uncertainty is a limit to engine operating range during the test. For the final analysis, a viable procedure for thrust stand calibrations, to allow a broader coverage of the engines operating envelope, was examined. The procedure for this calibration is shown in Appendix C, Table C.4 "+30K to -10K Calibration." The results are shown versus the conventional calibration in Figure 6 of Part 2. As seen in the figure, hysteresis is reduced by a small amount. Also, the loading to -10,000 lbf does not introduce curve-fit errors, as to the load vs. Tare curve used in data reduction, as great as those incurred for a conventional calibration loading to -30,000 lbf. For consistency, Analysis 5 will be compared to Analysis 1. Table 6 shows the values for Analysis 5. In comparison, the

Table 6. Results of Analysis 5 of Reduced Elemental Errors on Scale Force Uncertainty.

Note: Application to the 3,000 lbf Scale Force Measurement: +30K to -10K Calibration
with Reduced Hysteresis and Reduced Zero Shifts.

3K lbf Bias error

Table 1 item #	values, lbf	squares	sum of squares	sqrt of sum of squares, lbf
1a	1	1	538.2644	23.20052586
1b	2.5	6.25		
2		0		
3		0		
4		0		
5	5	25		
6		0		
7		0		
8		0		
9		0		
10	0.12	0.0144		
11		0		
12	1	1		
13	20	400		
14		0		
15	2	4		
16	10	100		
17	1	1		

3K lbf Precision error

Table 1 item #	values, lbf	squares	sum of squares	sqrt of sum of squares, lbf
1a		0	230.0036	15.16586958
1b		0		
2		0		
3		0		
4		0		
5		0		
6	15	225		
7	2	4		
8		0		
9		0		
10	0.06	0.0036		
11		0		
12		0		
13	0	0		
14		0		
15	1	1		
16		0		
17		0		

$U = [(23.2)^2 + (2(15.165))^2]^{.5} = 38.18$ lbf

hysteresis bias error 16 is reduced from 12 lbf to 10 lbf. The hysteresis precision error is reduced from 25 lbf to 15 lbf. The zero shift bias error 13 is now 20 lbf, and the precision error 13 is 0 lbf. These values resulted in a root-sum-square scale force uncertainty of 38.2 lbf or 1.27 % of 3,000 lbf. This uncertainty is slightly higher than in Analysis 4; however, more of the engine's operating envelope may now be covered during a test. This is very important to keep test efficiency high and test costs down.

Table 7 has been provided to summarize the numerical results obtained in the analysis of test calibration methodology and zero shifts on test data uncertainty. For comparison purposes, the uncertainty values obtained with both the additive and root-sum-square methodology are provided.

Table 7. Analysis Summary.

	range, lbf	B, lbf	S, lbf	Uadd, lbf	Urss, lbf	Uadd, %	Urss, %
Analysis 1	3000	40.327	29.928	100.183	72.173455	3.34	2.41
Analysis 2	3000	38.62	16.642	71.904	50.983616	2.40	1.70
Analysis 3	3000	24.13	25.1	74.33	55.698267	2.48	1.86
Analysis 4	3000	21.149	3.355	27.859	22.187931	0.93	0.74
Analysis 5	3000	23.201	15.165	53.531	38.186323	1.78	1.27

PART 4

CONCLUSION AND RECOMMENDATIONS

4.1 Summary

In summary, numerous factors affect the measurements which make up the elemental errors of scale force uncertainty. These elemental errors combine to result in total uncertainty of the desired measurement, the scale force produced by the engine. In this discussion, it was shown how hysteresis, thermal effects, and zero shifts contribute to scale force uncertainty. It was also noted that scale force was the primary contributor to thrust uncertainty in the low thrust (3,000 lbf) regions of engine operating envelopes. Thrust stand hysteresis was found to be controllable by the calibration procedure used. Zero shift effects were found to be controllable by better thrust stand service line installations together with controlling thermal effects by adhering to cell hardware temperature limits. Pre- to post-test zero shifts, which is a combination of hysteresis and thermal effects, were found to be controllable by also adhering to temperature limits. Therefore, scale force uncertainty can be reduced if care is taken to control the major elemental errors affecting the measurement.

4.2 Control of Hysteresis Effects

Hysteresis is controllable by the type of thrust stand calibration procedure used. For reduced hysteresis, calibrate the thrust stand to some applied load less than full scale. For example, calibrating the thrust stand to 10,000 lbf, where full scale is 50,000 lbf, will produce lower hysteresis. This method can be used effectively if the test period is dedicated to testing the engine in low thrust regions of its flight envelope, such as the

upper-left-hand corner of typical flight envelopes, where scale force levels are approximately 3,000 lbf. In most engine developmental programs, it is not feasible to dedicate a twenty hour test period to one region of the flight envelope. The selection of a thrust stand calibration procedure must therefore balance the uncertainty reductions achieved, versus the coverage of the flight envelope allowed by the various calibration procedures. This is important because engine test time is very expensive (approximately $25,000 per air-on hour) and test efficiency is critical to keep costs down. The author concludes, based on the results of the Analysis Summary (Table 7 of Part 3), that the calibration procedure of Analysis 5 be followed in a test program as the operating procedure for thrust stand calibrations. Analysis 5 utilized a +30K to -10K Thrust Stand Calibration. While Analysis 5 has the second best root-sum-square uncertainty level, it allows more coverage of an engine's flight envelope during testing, when compared to the load calibration procedure with the lowest uncertainty which was determined to be Analysis 4. As identified in Part 3, an uncertainty level of 1.27% of 3,000 lbf obtained in Analysis 5 is achievable only if additional operating restraints, to be identified next, are followed.

4.3 Control of Thermal Effects and Zero Shifts

Thermal effects are controllable by strict adherence to temperature limits set for the test environment and force measuring load cells. These effects cannot be quantified as such in a scale force uncertainty analysis; however, they are direct contributors to other

elemental errors. As previously discussed in the section on thermal effects, non-uniform thermal expansion of grounded service lines in the test environment directly affects scale force measurement. Several recommendations to control this growth include using maximum secondary cooling air (40-50% of engine airflow) at all times except when obtaining a performance type data point. Secondary cooling air should be kept to 10% or less [6] for performance data points. This cooling air is also important to help minimize thermal growth of the structural shell of the test cell, discussed earlier. Another recommendation to reduce thermal growth effects is to perform a directional audit on all service lines connecting the thrust stand and ground. All service lines should board the thrust stand in a direction perpendicular to the scale force measuring axis. A directional audit of the service lines will reveal abnormalities such as non-perpendicularity and provide the foundation for a service line history to be monitored by a test engineer. In minimizing thermal growth effects on test data quality, the cell temperature should be maintained at or below 100°F with a forward-aft delta of not more than 20°F.

The force measuring load cells are also sensitive to temperature fluctuations in the cell. The C1 Test Facility, where the experiments were performed, was designed with the load cells connecting the aft end of the thrust stand to the rear bulkhead, also called the aft support rings (see Figure 3). As described earlier, the rear bulkhead region of the test cell is subject to severe temperature gradients. The load cells are calibrated by the Precision Measurements and Equipment Lab at AEDC and contain a temperature correlation. However, through experience and "real world effects", electronic equipment

tends to be inconsistent over time and repeated exposure to high temperature (~200°F) conditions causes inconsistencies in the data. Force measuring load cells should be protected from thermal cycling and high temperatures by housing them in a water cooled enclosure and by using a radiation shield. Further, load cells should connect the thrust stand to ground in the front of the test cell near the cell anchor point. This is desirable for two reasons. First, the load cells will be in a more stable environment at the front of the test cell where they will be nearer the external cooling source and away from the engine exhaust. Secondly, the structural distortions caused by cell thermal growth is non-uniform, with the greatest growth and distortions of the test cell at the aft end. This is because the test cell is designed to thermally grow toward the exhaust duct. This has the potential to directly affect the system ground for the load cells because they are mounted in the rear of the test cell. In good practice, the load cells should be maintained to within ±10°F of their pre-test temperature reading.

Load cell zero shifts are a primary contributor to scale force uncertainty and can be controlled by adherence to cell operating temperature limits. Temperature limits identified in the section on hysteresis should be implemented to minimize service line growth and cell distortion effects that directly affect the data load train interaction with the thrust stand and ground. The important point here is to maintain pre-test cell environmental conditions as closely as possible throughout the test period. With these methods employed, zero shifts have been reduced to 20 lbf. Review Figure 7 to appreciate the benefits of properly operating and maintaining a thrust stand. The

importance of minimizing thermal gradients was also shown - Appendix F. The use of flex hose versus stainless steel tubing should be considered for each cell in order to reduce thermal growth contributions to zero shifts. Safety concerns may inhibit the use of flex hose; however, zero shift reductions can be realized due to the removal of rigid connections to the thrust stand. One final zero shift reducing method should also be identified here. If important performance data is to be acquired during a test period, an effective but costly procedure can be used. Shutting down the engine and performing the flex procedure is the first step. Next, acquire the performance data, shut the engine down, and perform the flex procedure once more. This brackets the critical data and effectively negates the zero shift. However, this procedure will take two hours of test time. It is a very effective method, yet costly, and should be left to the engine sponsor as to the need for such action.

4.4 Recommendations

In order to achieve the lowest possible scale force uncertainty, the following list of recommended actions should be considered for each test period:

1. Reduce hysteresis by tailoring the thrust stand calibration procedure to the test objectives to be accomplished in a particular test period.
2. Control and reduce cell thermal effects/zero shifts by:
    - Maintaining the cell environmental conditions at or below 100 °F.

- Maintaining the load cell temperature to within ± 10 °F of the pretest reading.
- Maintaining the forward-aft temperature delta in the test cell at or below 20 °F.
- Using maximum amounts of test cell cooling airflow (about 50% of engine airflow) except when obtaining performance data (where <10% should be used).
- Correctly routing all service lines perpendicular to the force measuring axis. The use of flex hose versus stainless steel tubing should also be considered where safety concerns allow.
- Mounting the force measuring system at the front of the test cell, away from the high temperature environment of the aft end. Protecting this system with a radiation shield and water cooled enclosure should also be performed.
- Shutting the engine down during a test and performing a flex, consistent with the calibration procedure selected, to obtain a mid-test zero load reading. This will "book-end" critical performance data and avoid any additional thermal growth effects that would occur as the test proceeds to other flight conditions.

3. Avoid data system effects by calibrating the instrumentation as close to the start of a test as possible. Following the suggestions in 2 above will also contain these effects.

REFERENCES

[1] Abernathy, Bob. In-Flight Thrust Determination and Uncertainty SP-674, UTSI Shortcourse sponsored by ASME. Warrendale, PA:1986.

[2] Adams, G.R. Improvement of Parameter Estimation through Uncertainty Analysis, New Orleans, LA: ASME 80-GT-9 (A80.42150), 1980.

[3] Covert, Eugene. Thrust and Drag: It's Prediction and Verification. AIAA vol.98, Progress in Astronautics and Aeronautics, 1985.

[4] Kline, S.J. "The Purpose of Uncertainty Analysis", ASME Journal of Fluids Engineering vol. 107, June 1985 pp 153.

[5] Moffatt, R.J. "Using Uncertainty Analysis in the Planning of an Experiment", ASME Journal of Fluids Engineering vol. 107, June 1985 pp 173.

[6] Wantland, E.C. and Mantone, A.J., Sverdrup Technology, Inc., AEDC Div., personal communication, 1997.

APPENDICES

GLOSSARY OF TERMS

Bias - The difference between the average of the measured samples of a given parameter and its true value.

Calibration - The process of comparing and correcting the response of an instrument to agree with a standard instrument over the measurement range.

Data Load Cell - A transducer for measuring the force transmitted through a data column.

Elemental Error - The bias and or precision error associated with a single component or process in a chain of components or processes.

Flex - The process of loading the thrust stand with the maximum possible thrust (positive) load and removing the load and applying the maximum possible drag (negative) load. Performed to ensure no binding of flexures.

Flexures - see **Service Lines**

Hysteresis - Greatest difference between the measured output at equal applied forces when one output is obtained by increasing the force from zero to full scale and the other by decreasing from full scale.

Measurement Error - The difference between the true value and the measured value. It includes both Bias and Precision errors.

Non-Linearity - The greatest deviation in measured output between any calibration points made with an increase in force from zero to full-scale force and a straight line drawn through the zero and full scale force outputs.

Precision - The closeness of agreement between repeated measurements.

Repeatability - Greatest deviation in the measured output when the same force is applied from the same direction under the same environmental conditions.

Service Lines - The pipe, tubing, conduit, cables etc. which carry fuel, power, control signals, or other services to the thrust stand or test article.

T_{95} - Ninety fifth percentile point for the two tailed student 't' distribution.

Tare - The difference between the test article force vector components and the forces reacted through the load cell, caused by service line stiffness, flexure restoring moment, and support column misalignment.

Tare Curve - The plot of the tare as the stand is flexed. The slope is used to correct data.

Thrust Stand - Test apparatus which supports engine.

Uncertainty - the maximum error one might reasonably expect for the defined measurement process.

Zero Repeatability - Any change in the zero unbalance after a load is applied and then removed

APPENDIX A
Theoretical Combination of Elemental Errors

Theoretical Combination of Elemental Errors

A measurement uncertainty is made up of a series of contributing elemental errors. These elemental errors must be combined to reflect the overall accuracy. If the individual elemental errors of a measurement are known, the total uncertainty can be estimated by application of the Taylor series. Consider the following discussion:

If N is a function of the independent measured quantities u_1, u_2, u_3, ..., u_n (and the u's are in error by $\pm\Delta u_1$, $\pm\Delta u_2$, $\pm\Delta u_3$, ..., $\pm\Delta u_n$) then the measurement errors will cause an error ΔN in the function N:

$$N = f(u_1, u_2, u_3, \ldots, u_n)$$

$$N \pm \Delta N = f(u_1 \pm \Delta u_1, u_2 \pm \Delta u_2, u_3 \pm \Delta u_3, \ldots, u_n \pm \Delta u_n)$$

If N is subtracted from the above expression to obtain an expression for $\pm \Delta N$, an approximate solution can be obtained by application of the Taylor series:

$$f(u_1 \pm \Delta u_1, u_2 \pm \Delta u_2, \ldots, u_n \pm \Delta u_n) = f(u_1, u_2, \ldots, u_n) + \Delta u_1 \partial f/\partial u_1$$

$$+ \Delta u_2 \partial f/\partial u_2 + \ldots + \Delta u_n \partial f/\partial u_n + \tfrac{1}{2}[(\Delta u_1)^2 \partial^2 f/\partial u_1^2 + \ldots] + \ldots$$

where all of the partial derivatives are evaluated at the known values of u_1, u_2, ..., u_n. In actual practice, the Δu's are small quantities, and thus the terms such as $(\Delta u)^2$ are negligible. Therefore, the equation can be approximated as:

$$f(u_1 \pm \Delta u_1, u_2 \pm \Delta u_2, \ldots, u_n \pm \Delta u_n) = f(u_1, u_2, \ldots, u_n) + \Delta u_1 \partial f/\partial u_1$$

$$+ \Delta u_2 \partial f/\partial u_2 + \ldots + \Delta u_n \partial f/\partial u_n$$

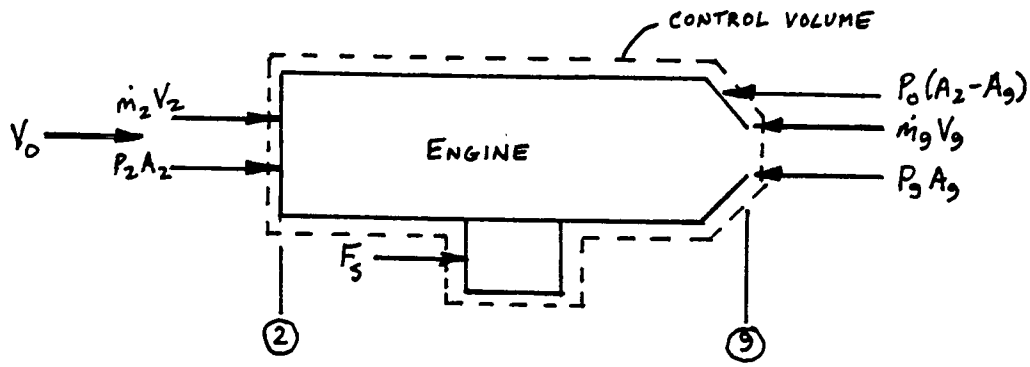
This gives the absolute error, E_a, as:

$$E_a = \Delta N = |\Delta u_1 \partial f/\partial u_1| + |\Delta u_2 \partial f/\partial u_2| + \ldots + |\Delta u_n \partial f/\partial u_n|$$

The absolute value sign is needed because some of the partial derivatives may be negative, and a positive value would reduce the total error. This approximation supplies an error value applicable to the function N and also shows which variables have the strongest influence on the accuracy of the measurement.

APPENDIX B
Definition of Thrust Terms

Definition of Thrust Terms



ASSUME: 1) $\dot{m}_{FUEL}$ IS NEGLIGIBLE
2) NO SKIN FRICTION

$$+\rightarrow \Sigma F_X = 0 \equiv F_S + \dot{m}_2 V_2 + A_2 P_2 - \dot{m}_9 V_9 - A_9 P_9 - P_0(A_2 - A_9)$$

$$0 \equiv F_S + \dot{m}_2 V_2 - \dot{m}_9 V_9 + A_2(P_2 - P_0) - A_9(P_9 - P_0)$$

$$F_G, \text{ Gross Thrust} = \dot{m}_9 V_9 + A_9(P_9 - P_0) = F_S + \dot{m}_2 V_2 + A_2(P_2 - P_0)$$

$$F_N, \text{ Net/Uninstalled Thrust} = F_G - F_{RAM}$$

$$\text{where } F_{RAM} = \dot{m}_2 V_0$$

$$\therefore F_N = \dot{m}_9 V_9 - \dot{m}_2 V_0 + A_9(P_9 - P_0) = F_S + \dot{m}_2 (V_2 - V_0) + A_2(P_2 - P_0)$$

$$\Rightarrow F_N = F_S + \dot{m}_2 (V_2 - V_0) + A_2(P_2 - P_0)$$

Definition of Thrust Terms (Continued)

I. Scale Force Term (F_S): The scale force term is defined as the reactive force imparted to the thrust stand as it is restrained from motion by its surrounding static structure. As can be seen from Figure 2, the static structure is the test cell. All direct contact between the thrust stand and the test cell is through the thrust measuring load cells. The load cells used in the C1 Test Facility are dual bridge strain gage load cells. The scale force is thus calculated by averaging the readings from these load cells.

II. Inlet Momentum/Drag Term ($m_2 (V_2 - V_0)$): The inlet momentum/drag term is defined as the product of the measured inlet airflow and the velocity differential of the air as it approaches the engine face in the inlet duct. Airflow is accurately calculated using an array of venturis. Inlet air velocity is calculated based on the inlet duct cross-sectional area and measured air temperatures and pressures within the duct.

III. A delta-P Term ($A_2(P_2 - P_0)$): The A delta-P Term represents the force acting on the engine due to the static pressure differential between the inlet air and the surrounding test cell environment. This term is calculated as the product of this pressure differential and the inlet ducting cross-sectional area.

All of the measurements which contribute to the thrust calculation have an uncertainty related to them. These individual uncertainties are called elemental errors and are combined to relate a total uncertainty on the measurement being performed. An elemental error due to a measurement can be anything from 1) tolerances on pressure measuring devices, 2) tolerances on temperature measuring devices, 3) physical limitations on the dimensional measuring devices, etc. Some elemental errors are more significant on uncertainty than others. Such is the case in thrust uncertainty calculation in areas of low thrust. Scale force uncertainty is the primary contributor to thrust uncertainty in these areas of low thrust. This paper will focus on minimizing the elemental errors associated with scale force measurement in an effort to achieve lowest possible uncertainty on thrust.

APPENDIX C
Thrust Stand Calibrations

TableC.1. Conventional Thrust Stand Calibration.

Procedural Steps of Calibration for Analyses 1 and 3

1. **Center the sliding lab seal.**
2. **Record steady state data point for zero reference.**
3. **Load thrust stand from 0K to 50K to -30K to 0K**
4. **Record steady state data point for zero reference.**
5. **Load the thrust stand as indicated below, a data point at each step.**

Note: The data points (DP) recorded are 10 second averaged values of the calibrate and data load cells. The data is obtained at 20 samples per second.

Conventional Thrust Stand Calibration	
DP	**LOAD**
501	**0K**
502	**10K**
503	**20K**
504	**30K**
505	**40K**
506	**50K**
507	**40K**
508	**30K**
509	**20K**
510	**10K**
511	**0K**
512	**-10K**
513	**-20K**
514	**-30K**
515	**-20K**
516	**-10K**
517	**0K**

5. **Recenter sliding lab seal.**
6. **Record Steady state data point for zero reference.**

Tabel C.2. 50K Thrust-Side-Only Calibration.

Procedural Steps of Calibration

1. **Center the sliding lab seal.**
2. **Record steady state data point for zero reference.**
3. **Load thrust stand from 0K to 50K to 0K lbf.**
4. **Record steady state data point for zero reference.**
5. **Load the thrust stand as indicated below, recording a data point at each step.**

Note: The data points (DP) recorded are 10 second averaged values of the calibrate and data load cells. The data is obtained at 20 samples per second.

50K Thrust-Side-Only Calibration	
DP	**LOAD (lbf)**
601	**0K**
602	**5K**
603	**10K**
604	**15K**
605	**20K**
606	**25K**
607	**30K**
608	**40K**
609	**50K**
610	**40K**
611	**30K**
612	**25K**
613	**20K**
614	**15K**
615	**10K**
616	**5K**
617	**0**

5. **Recenter sliding lab seal.**
6. **Record Steady state data point for zero reference.**

Table C.3. 10K Thrust-Side-Only Calibration.

Procedural Steps of Calibration for Analyses 2 and 4

1. **Center the sliding lab seal.**
2. **Record steady state data point for zero reference.**
3. **Load thrust stand from 0K to 10K to 0K lbf.**
4. **Record steady state data point for zero reference.**
5. **Load the thrust stand as indicated below, recording a data point at each step.**

Note: The data points (DP) recorded are 10 second averaged values of the calibrate and data load cells. The data is obtained at 20 samples per second.

10K Thrust-Side-only Calibration	
DP	LOAD (lbf)
601	0K
602	1K
603	2K
604	3K
605	4K
606	5K
607	6K
608	7K
609	8K
610	9K
611	10K
612	9K
613	8K
614	6K
615	4K
616	2K
617	0

5. **Recenter sliding lab seal.**
6. **Record Steady state data point for zero reference.**

Table C.4. +30K to -10K Thrust Calibration.

Procedural Steps of Calibration for Analysis 5

1. **Center the sliding lab seal.**
2. **Record steady state data point for zero reference.**
3. **Load thrust stand from 0K to 30K to -10K to 0K lbf.**
4. **Record steady state data point for zero reference.**
5. **Load the thrust stand as indicated below, recording a data point at each step.**

Note: The data points (DP) recorded are 10 second averaged values of the calibrate and data load cells. The data is obtained at 20 samples per second.

	+30K to -10K Thrust Calibration	
	DP	LOAD (lbf)
	601	0K
	602	5K
	603	10K
	604	15K
	605	20K
	606	25K
	607	30K
	608	25K
	609	20K
	610	15K
	611	10K
	612	5K
	613	0K
	614	-5K
	615	-10K
	616	-5K
	617	0

5. **Recenter sliding lab seal.**
6. **Record Steady state data point for zero reference.**

APPENDIX D
Curve-Fit Error

Curve-Fit Error

The curve-fit error, shown in Figure 8 on the following page, is obtained by normalizing the data for a thrust stand calibration through the use of a second-order curve. Figure 8 displays the actual thrust stand calibration data points and the resulting curve-fit. In the present analysis of scale force uncertainty, the 3,000 lbf level of FAC is where the error must be identified. The actual lbf number to be used in the scale force uncertainty analysis for a curve-fit error is identified by averaging the two data points at 3,000 lbf obtained from the calibration and calculating the difference versus the corresponding value obtained from the slope of the curve-fit line. Over the course of a test program, a thrust stand calibration is performed for each test period. From these calibrations, the maximum value of the curve-fit error realized is then used in the scale force uncertainty calculation. This curve-fit error is directly influenced by the magnitude of hysteresis and the non-linearity of the data obtained from the thrust stand calibration. The results presented in Part 3 convey the importance of minimizing the hysteresis, and thus the non-linearity due to installation effects, when attempting to reduce scale force uncertainty.

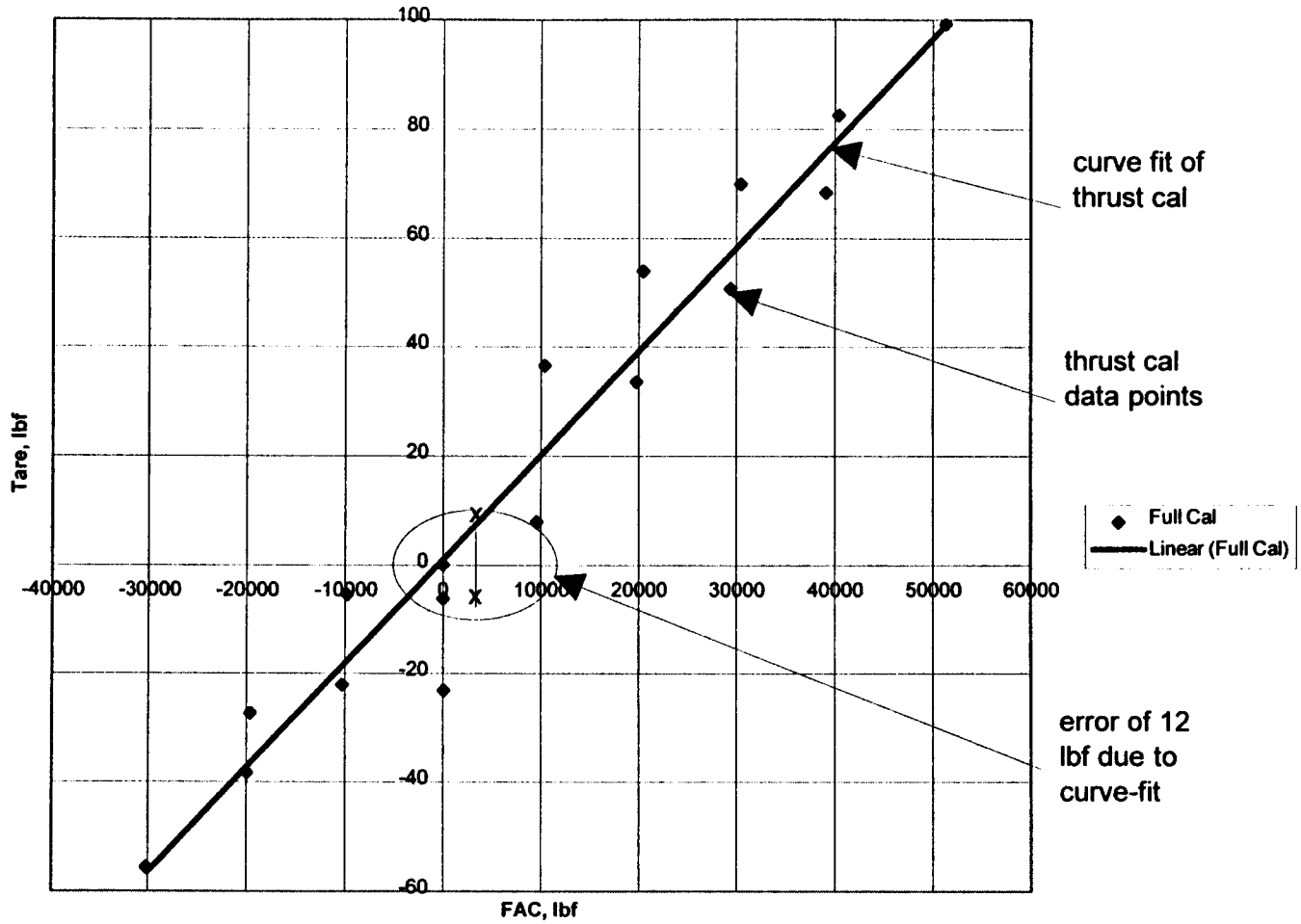


Figure 8. Curve-Fit Error

APPENDIX E
Zero Shift Error

Zero Shift Error

The zero shift error, shown in Figure 9 on the following page, is identified as the difference between zero load readings of the pre- and post-test flex procedures. The zero load points are obtained after the pre- and post-test flex procedures, the flex procedures being consistent with the type of calibration procedure used. This difference in zero load readings is used to add to or subtract from the scale force data obtained during a test period. In the application to scale force uncertainty, the zero shifts (for all test periods in a test program) are averaged to obtain the bias for this error. The standard deviation of these zero shifts is used as the precision for this error. Thus the zero shift bias and precision errors reflect the measurement accuracy of scale force for an entire test program. The important point to note from Figure 9 is that the slope of the tare curve is unchanged, only the zero load point has shifted. Remember that tare is defined as the difference in input force and measured force on a thrust stand. The shift in the zero load point is the result of thermal growth influencing the measured force reading. Therefore, when a zero shift is realized pre- to post-test, the only difference is that thermal growth has caused forces to be imparted to the thrust stand that were not there in the pre-test data.

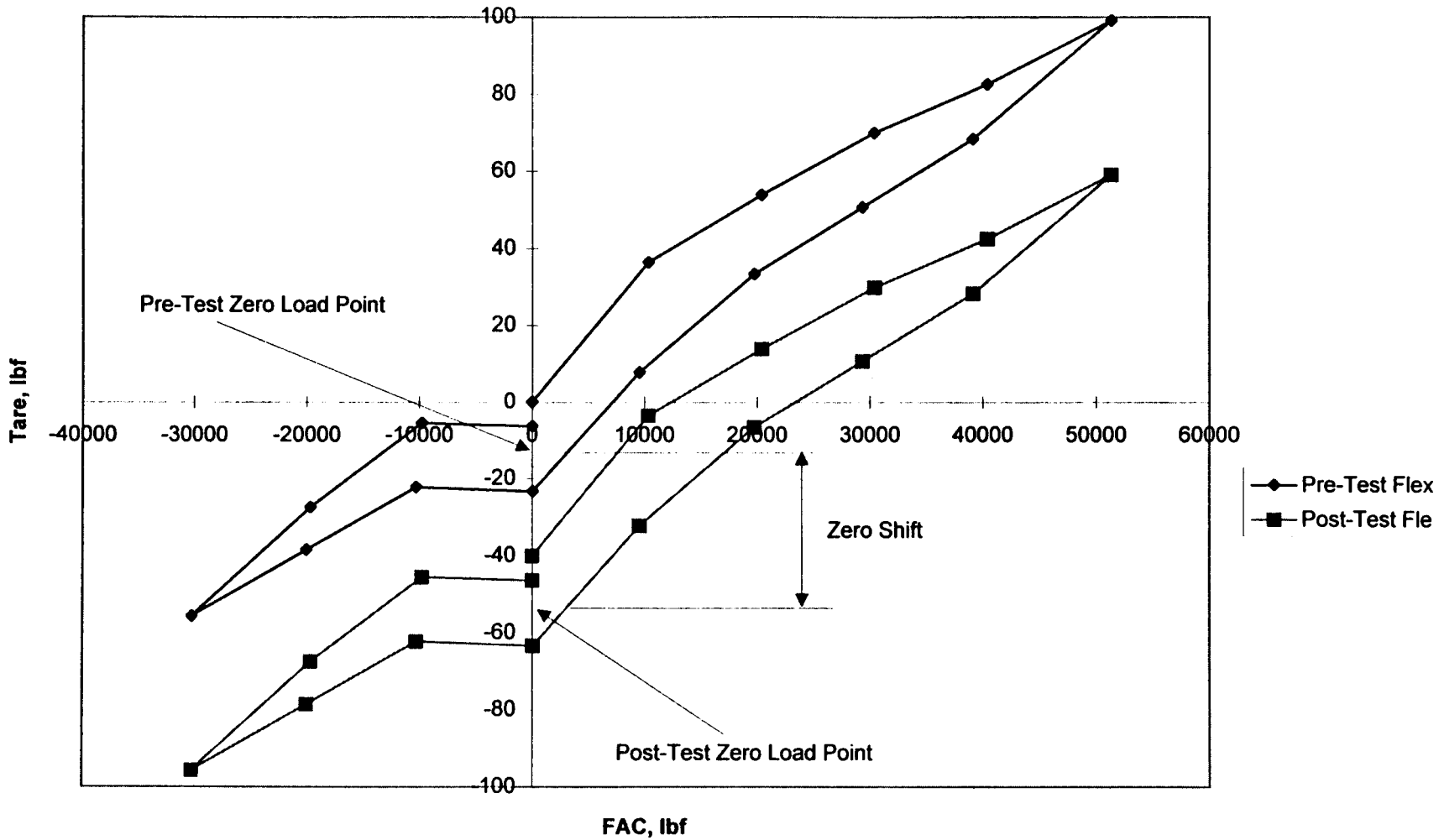


Figure 9. Zero Shift Error

APPENDIX F
Implications of Thermal Growth of Test Cell on Zero Shifts

Implications of Thermal Growth of Test Cell on Zero Shifts

Elongation of Test Cell due to temperature gradient:

Assume: -test cell constructed of AISI 1020 Steel with $\alpha = 6.5 \times 10^{-6}/°F$
-test cell is 50 feet in length

I. Temperature Gradient of 80°F:

$\zeta = \alpha L \Delta T$
$= (6.5 \times 10^{-6}/°F)(50 \text{ ft})(12 \text{ in}/1 \text{ ft})(80 °F)$
$= .312 \text{ in}$

II. Temperature Gradient of 50°F:

$\zeta = \alpha L \Delta T$
$= (6.5 \times 10^{-6}/°F)(50 \text{ ft})(12 \text{ in}/1 \text{ ft})(50 °F)$
$= .195 \text{ in}$

This thermal growth represents a relative displacement between the test cell (ground) and the thrust stand. This relative displacement creates a restoring force in the service lines connecting the test cell and the thrust stand.

Estimate for load placed on thrust stand from service lines due to thermal growth of test cell:

Assume: -service lines are schedule 40 stainless steel tubing
-Modulus of Elasticity = $30 \times 10^6 \text{ lb/in}^2$
-service lines are modeled as fixed-free columns (cantilevered beam) with applied load at free end. This assumes the thrust stand applies the load.

I. A. ¾ inch diameter service line with Moment of Inertia (I) = 0.037 in^4, temperature gradient of 80°F:

$F = y3EI/L^3$
$= (.312 \text{ in})(3)(30 \times 10^6 \text{ lb/in}^2)(0.037 \text{ in}^4) / ((50 \text{ ft})(12 \text{ in}/1 \text{ ft}))^3$
$= 0.82 \text{ lbf}$

B. ¾ inch diameter service line with Moment of Inertia (I) = 0.037 in^4, temperature gradient of 50°F:

$F = y3EI/L^3$
$= (.195 \text{ in})(3)(30 \times 10^6 \text{ lb/in}^2)(0.037 \text{ in}^4) / ((50 \text{ ft})(12 \text{ in}/1 \text{ ft}))^3$
$= 0.52 \text{ lbf}$

Implications of Thermal Growth of Test Cell on Zero Shifts (Cont.)

II. A. 1 inch diameter service line with Moment of Inertia (I) = 0.0874 in^4, temperature gradient of 80°F:

$$F = y3EI/L^3$$
$$= (.312\ in)(3)(30 \times 10^6\ lb/in^2)(0.0874\ in^4) / ((50\ ft)(12\ in/1\ ft))^3$$
$$= 1.95\ lbf$$

B. 1 inch diameter service line with Moment of Inertia (I) = 0.0874 in^4, temperature gradient of 50°F:

$$F = y3EI/L^3$$
$$= (.195\ in)(3)(30 \times 10^6\ lb/in^2)(0.0874\ in^4) / ((50\ ft)(12\ in/1\ ft))^3$$
$$= 1.22\ lbf$$

The resulting forces (restoring) placed on the thrust stand will cause a zero shift. This is due to the fact that these forces were not accounted for in pretest data because the cell was at ambient temperature and thus no thermal gradients.

Total possible force input to thrust stand due to thermal growth:

There are approximately 1000 service lines in the C1 Test Facility which connect the test cell (ground) and the thrust stand. These service lines vary in size from ¼ inch to 3 inch in diameter. For simplicity, all service lines will be modeled as the equivalent of 50 - ¾ inch lines and 20 - 1 inch lines.

I. Total force due to temperature gradient of 80°F:

$$F = 50(0.82\ lbf) + 20(1.95\ lbf)$$
$$= 79\ lbf$$

II. Total force due to temperature gradient of 50°F:

$$F = 50(0.52\ lbf) + 20(1.22\ lbf)$$
$$= 50.4\ lbf$$

The force imparted to the thrust stand due to thermal growth is a major contributor to zero shifts. Additionally, zero shifts are the primary elemental error affecting scale force uncertainty. As a result, it is imperative that thermal gradients in the test cell be minimized.

Vita

Gregory Darin Hollis was born in Tullahoma, Tennessee on March 6, 1971. He attended schools in the public system of Tullahoma, Tennessee, the Tullahoma City School System, where he graduated from Tullahoma High School in May, 1989. He attended Middle Tennessee State University, Murfreesboro, Tennessee from August of 1989 to May of 1991. He then transferred to Tennessee Technological University, Cookeville, Tennessee in August of 1991 where in December, 1993 he received the Bachelor of Science degree in Mechanical Engineering. After graduation, he began work for Sverdrup Technology at Arnold Engineering and Development Center on Arnold Air Force Base, Tullahoma, Tennessee. While-and-after working on various engine altitude development programs, he entered the Master's program in Mechanical Engineering at The University of Tennessee Space Institute, Tullahoma in January of 1994, officially receiving the Master's degree in December, 1997.

He is presently working in the Large Turbine Engine Group at Arnold Engineering and Development Center as Project Engineer for the Sea Level Environmental Test Cells.